Astragalosides IV Improves Palmitic Acid-induced Renal Tubular Epithelial Cells Injury Due to Inhibition of NLRP3 Inflammasome

Yanhua Zhang
Anhui Medical University
Yan Li
Anhui Medical University
Yong Su
The First Affiliated Hospital of Anhui Medical University
Yunfeng Zhu
Anhui Medical University
Yuli Han
Anhui Medical University
Xianan Dong
Anhui Medical University
Weizu Li (liweizu@126.com)
Anhui Medical University https://orcid.org/0000-0002-8305-1414
Weiping Li
Anhui Medical University

Research

Keywords: Astragaloside IV, Renal tubular epithelial cells, NADPH oxidase 4 (NOX4), NLRP3 inflammasome, Diabetic nephropathy

DOI: https://doi.org/10.21203/rs.3.rs-122884/v1

Abstract

Background

Diabetic nephropathy (DN) is a serious complication of type 2 diabetes mellitus (T2DM). Hyperlipidemia plays a key role in occurrence and development of DN. The main saturated fatty acids of palmitic acid (PA) is closely related to glomeruli and tubules injury in T2DM. Astragaloside IV (AS-IV) has comprehensive pharmacological effects, such as anti-inflammation, anti-oxidation and anti-apoptosis. However, whether AS-IV can attenuate PA-induced renal tubular epithelial cells damages and its underlying mechanisms remain unclear.

Methods

In vitro, the HK-2 cells were stimulated with PA (200 μM) for 6, 9, 12, and 24 h respectively, then treated with AS-IV (10, 20 or 40 μM) and Apo (100 μM) for 24 h. In vivo, we investigated the effects of AS-IV in high-fat diets (HFD) and low-dose streptozotocin (STZ)-induced type 2 DN rats. Cell viability was detected by Cell Counting Kit-8 (CCK-8) assay kit. The lipid deposition was detected by ORO Staining assay kit. Annexin V-FITC/PI staining was used to detect the cell apoptosis. Immunofluorescence staining and Immunohistochemistry were used to measure the expressions of NLRP3 and NOX4. The ELISA kits were conducted to assess the levels of IL-1β, IL-18, GSH and SOD. Western blotting was used to assess the expressions of NLRP3, caspase-1, ASC, 1L-1β, NOX4, p22phox and p47phox proteins.

Results

Our results indicated that PA exposure not only significantly decreased cell viability, GSH and SOD expressions, and increased lipids deposition and apoptosis, but also increased the level of ROS and the expressions of IL-1β and IL-18. Moreover, PA exposure significantly increased the expressions of NADPH oxidase 4 (NOX4), NLRP3, ASC and caspase-1. However, all these abnormalities were significantly ameliorated by AS-IV and apocynin (Apo) treatment. In addition, our results indicated that AS-IV (80 mg/kg) could attenuate the renal tubular pathological injury and lipids deposition, and decrease the expressions of NLRP3, ASC, caspase-1, NOX4, p22phox and p47phox in renal tubules.

Conclusions

The study suggested that AS-IV could improve PA-induced HK-2 cells injury and renal tubular damage in T2DM rats, and the mechanism may be related to inhibition of NOX4-mediated NLRP3 inflammasome activation.

1. Background

Diabetic nephropathy (DN) is a lethal complication of diabetes mellitus and has become a major cause of end-stage renal disease. Although numerous studies have focused the lesions of DN mainly on glomerulosclerosis, more and more studies indicated that diabetic renal damage also occurs in the renal

tubules [1, 2]. Increasing evidences demonstrate that renal tubular epithelial cells injury is also an important characteristic of DN, and apoptosis of renal tubular epithelial cells is observed in mice, rats and humans with DN [3]. In addition to hyperglycemia, high levels of free fatty acids (FFAs) are also observed in type 2 diabetes mellitus (T2DM) and have been identified as a risk factor of DN [4]. Recent studies indicated that high levels of FFAs are involved in DN by inducing endoplasmic reticulum stress and oxidative stress, and leading to podocyte apoptosis [5]. Clinical studies have found that many patients with DN have obvious dyslipidemia [6, 7]. Palmitic acid (PA) is a major lipid derivative in human body, and it has been reported that the lipotoxicity induced by PA can cause human kidney-2 (HK-2) epithelial cell to produce oxidative stress, inflammation, fibrosis and apoptosis, thereby inducing renal dysfunction and aggravating DN [8]. However, the specific mechanism of PA-induced renal tubular damage has not yet been elucidated.

Oxidative stress and inflammation play important roles in the pathological damage of renal tubules. Excessive ROS production can induce oxidative stress and inflammation, and promote the renal tubular cells damage, resulting in renal injury [9]. NADPH oxidase (NOX) is a constitutively multi-subunit enzyme that acts as an oxygen sensor and an electron donor to generate ROS from molecular oxygen. NOX4, one subtype of NOX in kidney, contributes to the ROS accumulation in kidney diseases including DN [10, 11]. Increasing researches have indicated that NOX4 is involved in the damage of HK-2 cells, leading to mesenchymal transition, apoptosis and inflammation [12, 13]. Moreover, it has been reported that DN may be an inflammatory disease [14]. Inflammasomes play a central role in cleaving procaspase-1 to caspase-1, which eventually leading to the generation of proinflammatory factors [15]. The subtype of NLRP3 inflammasome is widely expressed in the glomerulus and renal tubules [16]. It has been reported that NLRP3 inflammasome plays an important role in renal injury and closely involves in the pathogenesis of DN, acute and chronic kidney disease [17, 18]. Over activation of NLRP3 inflammasome participates in the damage of renal tubular epithelial cells by releasing mature inflammatory factors [19]. ROS is one of the important factors for activation of inflammasome, and more and more evidence shows that NOX4 and NLRP3 inflammasome can regulate each other and play a role together in various kidney injuries [20, 21]. Our previous works showed that PA exposure could significantly induce ROS accumulation in HK-2 cells [22]. Therefore, we hypothesized that NOX4-mediated activation of NLRP3 inflammasome may be involved in PA-induced HK-2 cells injury.

At present, there are few medicines for treatment of DN. Astragaloside IV (AS-IV) is extracted from traditional Chinese medicinal plant Astragalus membranaceus. In recent years, various pharmacological effects of AS-IV have been reported, such as anti-oxidative stress, anti-inflammatory, anti-apoptosis and anti-fibrosis in vivo and in vitro [23]. Growing evidence has shown that AS-IV can improve DN rats through antioxidant and anti-inflammatory mechanisms. Additionally, AS-IV can also inhibit high glucose-induced HK-2 cells apoptosis through inhibiting oxidative stress [1]. Our previous work indicated that AS-IV could also alleviate PA-induced HK-2 cells injury [22]. However, whether AS-IV can protect against kidney tubule injury by inhibition of NOX4-mediated NLRP3 inflammasome activation is still unknown. This study was performed to study the potential protective effect and mechanism of AS-IV on PA-induced HK-2 cells

injury and on kidney tubular damage in T2DM rats. This research may provide potential targets for the prevention of DN.

2. Materials And Methods

2.1 Cell culture and treatment

Human kidney 2 (HK-2) is a proximal tubular cell line derived from normal kidney. HK-2 cells were cultured in DMEM/F12 medium containing 10% fetal bovine serum, 100units/ml penicillin and 100 μg/ml streptomycin at 37 °C with 5% CO_2. The experiments were divided into two parts. In the first part, the HK-2 cells were treated with PA (200 μM) for 6, 9, 12, and 24 h respectively to study the effect and mechanism of PA on tubular cells injury. In the second part, to study the protective effect and mechanism of AS-IV on PA-induced tubular cells injury, the HK-2 cells were divided into six groups: (1) control group, the cells were cultured with 0.2% BSA; (2) model group, the cells were treated with PA (200 μM) for 24 h; (3–5) AS-IV groups, the cells were treated simultaneously with PA (200 μM) and AS-IV (10, 20 or 40 μM) for 24 h; (6) apocynin (Apo) group, the cells were treated simultaneously with PA (200 μM) and Apo (100 μM) for 24 h.

Palmitate (PA, sigam-aldrich, USA) was prepared as previously reported method [22]. Briefly, PA (27 mM) was dissolved in distilled water (70℃) for 30 min. The bovine serum albumin (BSA, 30%; Shanghai Yeasen Biotechnology Co., Ltd, China) was also dissolved in distilled water (55℃) for 30 min. Then the PA and BSA solution were mixed at a molar ratio of 6:1 and stored at 4℃ as a storage solution. Astragaloside IV (AS-IV, ≥ 98%, Nanjing Zelang Pharmaceutical Technology Co.) and apocynin (Apo, Merck Millipore) were dissolved in DMSO as a stock solution stored at -20℃. When using, the stock solution was diluted with DMEM with final DMSO concentration less 0.5% (v/v).

2.2 Animals and treatment

The Sprague-Dawley rats (male, 180–220 g) were obtained from the Shandong Experimental Animal Center. The animals (40 rats) were randomly divided into two groups: control group (10 rats), maintained with standard diet for 8 weeks; High fat diet group (HFD, 30 rats), fed with HFD (59.5% standard diet, 20% sucrose, 10% yolk powder, and 10% lard) for 8 weeks.

Eight weeks later, the HFD rats were administrated with a single intraperitoneal injection of streptozotocin (STZ, 35 mg/kg, Shanghai Yuanye Biotechnology Co., Ltd. Shanghai, China), which was dissolved in the citrate buffer (pH 4.6, 0.1 M). After 72 hours, the blood glucose concentrations were detected with a Roche blood glucose meter from the tail vein. The rats (blood glucose concentration ≥ 16.7 mmol/L) were divided randomly into three groups (n = 10): model group, AS-IV group (80 mg/kg) and Metformin (Met, 200 mg/kg) groups, and continued to be fed with HFD. AS-IV and Metformin (Shanghai Shangyao Xinyi Pharmaceutical Co., Ltd.) were suspended in carboxymethyl cellulose sodium (0.5%) and were treated intragastrically once a day. The normal control group and the model group were treated with equal volume of solvent. All animal experiments were approved by the Institutional Ethics Committee of Anhui Medical University.

2.3. Cell viability assay

Cell Counting Kit-8 (CCK-8) assay kit (Dojindo, Kumamoto, Japan) was used to assess cell viability. The cells (5×10^3 per well) were seeded in 96-well plate. The CCK-8 solution (10%) was added to the media and continuously incubated for 2 h. The optical density (OD, 450 nm) of each well was detected using a microplate reader (Thermo Fisher Company, USA). Cell viability = (administration group OD - blank group OD) / (control group OD - blank group OD) × 100%.

2.4. Oil Red O (ORO) staining of HK-2 cells

The cellular lipid deposition was detected by ORO Staining assay kit (Solarbio, Beijing). The cells were washed twice with PBS and then fixed with ORO Fixative for 30 min. Then cells were washed twice with water and immersed in 60% isopropyl alcohol for 5 min. Afterwards, the cells were immersed in ORO Stain for 20 min and washed with water, and visualized by using a microscope (BX-51, Olympus Co., Ltd. Japan). The mean density of lipid deposition in each group were quantified by using Image-Pro Plus 6.0 software.

2.5. Apoptosis analysis of HK-2 cells

Annexin V-FITC/PI staining was used to detect the cell apoptosis by a commercial kits (Beibo Biology Co., Ltd. Shanghai, China). Briefly, the cells were suspended with 400 μL of 1 × binding buffer to make the cell concentration approximately 1×10^6 cells/ml. Then the cells were incubated with Annexin V-FITC and PI for 15 minutes in darkness at 2–8℃. Flow cytometry (BD Biosciences, USA) was used for analysis, and apoptotic HK-2 cells (Annexin V^+/PI^-) were shown in the lower right quadrant.

2.6. ROS production assay

For ROS assay, HK-2 cells were incubated with H2DCFDA (KeyGEN, Jiangsu, China, 5 μM) for 30 min at 37℃ in darkness. The nonfluorescent H2DCFDA can be oxidized into DCF to generate fluorescence by the existing peroxides, hydroperoxides, etc. after entering the cell. The results were examined by using a fluorescence microscopy (Olympus IX71, Japan). The mean fluorescence density of each group was analyzed by using the Image Pro Plus 6.0 software to assess the production of ROS.

2.7. Immunofluorescence staining

The cells were cultured in 24-well plates. For examination, the cells were washed three times with PBS, and then fixed with paraformaldehyde (4%) for 30 min. After that, cells were permeabilized with 10% Triton X-100 for 30 min and blocked with 3% BSA for 30 min. Primary antibody against NLRP3 (1:200) was incubated overnight at 4℃, followed by incubation with a fluorescent secondary antibody. Then cells were washed by PBS and stained nucleus with DAPI for 5 min. The positive areas were examined by using a microscopy (Olympus IX71, Japan). The mean fluorescence density of each group was performed by using the Image Pro Plus 6.0 software to indicate the expression of NLRP3.

2.8. Enzyme-linked immunosorbent assay (ELISA)

The ELISA kits (MEIMIAN, Jiangsu, China) were conducted to assess the levels of interleukin IL-1β and IL-18 in cultured supernatants, and GSH, SOD in cells protein according to the protocols. All human ELISA kits had high sensitivity and excellent specificity for detection of IL-1β, IL-18, GSH and SOD with no significant cross-reactivity or interference being observed.

2.9. Immunoblotting analysis

Total proteins were extracted from HK-2 cells and renal cortex homogenate of T2DM rats. The proteins concentration was detected by using a BCA kit (Beyotime biotechnology, Shanghai, China). The same amount of proteins was separated by 8–15% SDS-PAGE, then the proteins were transferred to a PVDF membrane. After that, the PVDF membrane was blocked with 5% skim milk in TBST for 1 h, then the membrane was washed with TBST three times and incubated overnight at 4℃ with corresponding primary antibodies of anti-NLRP3 (Zenbio, 381207, 1:1000), anti-caspase-1 (Affinity, AF5418, 1:1000), anti-ASC (Bioss, BS6741R, 1:1000), anti-NOX4 (Affinity, DF6924, 1:1000), anti-p22phox (Bioworld, BS60290, 1:1000), anti-p47phox (Affinity, AF5220, 1:1000), anti-IL-1β (Bioworld, BS3506, 1:1000), anti-GAPDH (Affinity, AF7021, 1:3000). The next day, the membrane was washed with TBST and incubated with a HRP-conjugated secondary antibody (1:10000) at room temperature for 1 h. Lastly, ECL was used to visualize and observe the expression of proteins by using a Bioshine Chemi Q4600 Mini Imaging System (Shanghai Bioshine Technology, China). And semi-quantitative analysis was manipulated by using the image J software. The gray value of protein band was normalized to the corresponding GAPDH band.

2.10. HE and Oil Red O staining of kidney tissues

The T2DM rats were sacrificed and the kidneys were removed immediately. One kidney was kept in -80 ℃, and the other was fixed with paraformaldehyde (4%). For HE staining, the kidney specimen was embedded in paraffin, and cut into 5 μm thick sections. The paraffin sections conventional dewaxing to water and stain with hematoxylin and eosin (HE). For Oil Red O staining, kidney specimen was embedded in the OTC and cut into 10 μm sections with a frozen slicer (Leica CM3050, Germany). Kidney sections were stained with Oil Red O solution for 8–10 min, and observed under an optical microscope (Olympus IX71, Japan). The density of positive area in each group was analyzed with Image-Pro Plus 6.0 analysis software to quantify the lipid deposition.

2.11. Immunohistochemistry

Kidney sections were deparaffinized and rehydrated, then were placed in sodium citrate buffer (pH6.0) with a microwave oven heating for 10 min to repair antigen. Then the slides were incubated with 3% hydrogen peroxide solution for 25 min, then were blocked with 3% BSA for 30 min. Primary antibodies of NLRP3 (Affinity, DF7438, 1:50) and NOX4 (Service bio, GB11347, 1:100) were added to the sections, and the sections were placed in a wet box and incubated at 4℃ overnight. Then the tissues were covered with secondary antibody (Affinity, S0001, 1:500) and incubated at room temperature for 50 min. Subsequently, DAB chromogen (Service bio, G1211) was used and the nucleus was counter stained with hematoxylin.

The intensity of positive areas was analyzed by using Image-Pro Plus 6.0 analysis software to assess the expressions of NLRP3 and NOX4 in kidney tubules.

2.12. Statistical analysis

The data were analyzed using Graph Pad Prism 6 (Graph Pad Software, San Diego, CA, USA). The results were expressed as mean ± SD. Differences among groups were calculated using one-way analysis of variance (ANOVA), then followed by *t*-test to compare the differences between groups. $P < 0.05$ is defined as statistically significant.

3. Results

3.1. AS-IV increases cell viability in PA-induced HK-2 cells

To detect PA-induced cells injury and the effect of AS-IV on PA-induced HK-2 cells, PA (200 μM) was used to stimulate the cells for 6 h, 9 h, 12 h and 24 h, and AS-IV (10, 20 and 40 μM) and Apo (100 μM) were used to intervene for 24 h. The results showed that the longer the PA induction, the lower the cell viability was observed as compared with BSA control group, especially in 24 h (Fig. 1A, $P < 0.01$). However, AS-IV (10, 20 and 40 μM) and Apo treatment for 24 h significantly increased cell viability in PA-induced HK-2 cells as compared with the model group (Fig. 1B, $P < 0.01$). The results suggested that AS-IV treatment could alleviate PA-induced HK-2 cells injury.

3.2. AS-IV attenuates lipid deposition in PA-induced HK-2 cells

Excessive lipid deposition in cells can cause lipotoxicity. To evaluate the effects of PA and AS-IV on cell lipid deposition, the Oil Red O Staining was performed in PA-induced HK-2 cells. As shown in Fig. 2A and B, the intracellular lipid deposition was significantly increased in HK-2 cells with the prolongation of PA exposure as compared with BSA control group ($P < 0.01$). As shown in Fig. 2C and D, AS-IV (10, 20 and 40 μM) and Apo treatment for 24 h significantly decreased lipid deposition in PA-induced HK-2 cells as compared with the model group ($P < 0.01$). The data suggested that AS-IV treatment could significantly alleviate PA-induced lipotoxicity in HK-2 cells.

3.3. AS-IV reduces apoptosis in PA-induced HK-2 cells

The renal tubular epithelial cells apoptosis also plays important roles in the pathogenesis of DN. To observe the effect of AS-IV on PA-induced HK-2 cells apoptosis, the cells were subjected to apoptosis assay by using Annexin V-FITC/PI Kits and were detected by flow cytometry. The results showed that the apoptosis rate was significantly increased with prolongation of PA exposure compared with BSA control group, especially in 12 h and 24 h (Fig. 3A and B, $P < 0.05$). However, as shown in Fig. 3C and D, AS-IV (20

and 40 μM) and Apo treatment significantly decreased the apoptosis rate in PA-induced HK-2 cells (P< 0.01). The results suggested that AS-IV treatment could inhibit PA-induced HK-2 cells apoptosis.

3.4. AS-IV decreases ROS generation in PA-induced HK-2 cells

The lipotoxicity caused by excessive lipid deposition can induce oxidative stress in the body. Therefore, we further performed H2DCFDA staining to evaluate PA-induced ROS accumulation in HK-2 cells. As shown in Fig. 4A and B, the results showed that the ROS level was significantly increased with increase of PA exposure time compared with BSA control group (P< 0.05 or P< 0.01). We also observed the effect of AS-IV and Apo treatment on PA-induced ROS accumulation in HK-2 cells. The results showed that AS-IV (10, 20 and 40 μM) and Apo could significantly decrease ROS accumulation in PA-induced HK-2 cells (Fig. 4C and D, P< 0.01). The results suggested that AS-IV treatment could decrease ROS accumulation in PA-induced HK-2 cells.

3.5. AS-IV decreases GSH, SOD expressions in PA-induced HK-2 cells and IL-1β, IL-18 levels in supernatant

To assess the redox state and inflammation in PA-induced HK-2 cells and the protective effect of AS-IV, we further detected the GSH and SOD expressions in HK-2 cells, and the IL-1β, IL-18 levels in supernatant by ELISA. Our results indicated that PA exposure for 6, 9, 12 and 24 h significantly decreased the expressions of GSH and SOD in HK-2 cells, and increased the IL-1β and IL-18 levels in supernatant compared with BSA control group (Fig. 5A, B, E and F, P< 0.05 or P< 0.01). On the contrary, after administration with AS-IV and Apo for 24 h, the GSH and SOD expressions were significantly increased in HK-2 cells, and theIL-1β and IL-18 levels in supernatant were significantly decreased compared with PA-induced model group (Fig. 5C, D, G and H, P< 0.05 or P< 0.01). The results suggested that PA exposure could decrease the antioxidant function and increase inflammation in HK-2 cells, while AS-IV treatment could improve oxidative stress and inflammation in PA-induced HK-2 cells.

3.6. AS-IV downregulates expressions of NLRP3, caspase-1, ASC, IL-1β and NOX4 in PA-induced HK-2 cells

NOX4 is an important enzyme contributing to ROS generation, which can further activate NLRP3 inflammasome. We further used immunoblot analysis to confirm whether NOX4 and NLRP3 inflammasome are involved in PA-induced redox imbalance and inflammation in HK-2 cells. The results showed that PA exposure for 6, 9, 12 and 24 h could significantly increase the expressions of NLRP3, ASC, caspase-1 and NOX4 in HK-2 cells compared with BSA control group (Fig. 6A-E, P < 0.05 or P< 0.01). AS-IV (10, 20, and 40 μM) and Apo (100 μM) treatment for 24 h significantly decreased the expressions of NLRP3, caspase-1, ASC and NOX4 in HK-2 cells compared with PA-induced model group (Fig. 6F-J, P < 0.05 or P< 0.01). These data suggested that NOX4 and NLRP3 inflammasome activation closely involved

in PA-induced HK-2 cells injury, and AS-IV treatment could inhibit NOX4 and NLRP3 inflammasome activation and protect against PA-induced HK-2 cells damage.

To further confirm the protective effect of AS-IV on PA-induced NLRP3 inflammasome activation, we also examined the expression of NLRP3 by immunofluorescence. The results indicated that PA stimulation significantly increased the expression of NLRP3 in HK-2 cells compared with BSA control group. Meanwhile, AS-IV and Apo treatment could decrease NLRP3 expression compared with model group (Fig. 7A and B, $P < 0.01$).

3.7. AS-IV alleviates renal histopathology and lipid deposition in T2DM rats

To confirm the effect of AS-IV on kidney tubular injury, we examined the renal histopathology and lipid deposition in T2DM rats. The HE staining results indicated that the renal tubules showed significant vacuolar degeneration and enlarged lumenin in the T2DM model group as compared with control group. And AS-IV (80 mg/kg) and Met (200 mg/kg) treatment for 8 weeks significantly improve these pathological changes as compared with model group (Fig. 8A). In addition, Oil red O staining was used to detect the lipid deposition in the kidney. As shown in Fig. 8B and C, the lipid deposition was significantly increased in the T2DM model rats as compared with the control group. And AS-IV (80 mg/kg) and Met (200 mg/kg) treatment for 8 weeks significantly decreased the lipid deposition as compared with model group. The data suggested that AS-IV treatment could alleviate the renal tubular histopathology and lipid deposition in T2DM rats.

3.8. AS-IV downregulates NLRP3 and NOX4 expressions in renal cortex of T2DM rats

To further assess the effect of AS-IV treatment on NLRP3 inflammasome and NOX4 activation in T2DM rats, we detected the expressions of NLRP3 and NOX4 related proteins in the renal cortex by using immunoblotting. The results showed that the expressions of NLRP3, caspase-1, ASC, IL-1β, NOX4, p22phox, and p47phox were significantly increased in the T2DM model rats compared with control group (Fig. 9, $P < 0.01$). And AS-IV (80 mg/kg) and Met (200 mg/kg) treatment for 8 weeks significantly decreased the expressions of NLRP3, caspase-1, ASC, IL-1β, NOX4, p22phox and p47phox in renal cortex of the T2DM rats compared with model group (Fig. 9, $P < 0.05$ or $P < 0.01$).

To further demonstrate the effect of AS-IV on NLRP3 and NOX4 expressions in renal tubules, the immunohistochemistry was performed to detect the expressions of NLRP3 and NOX4. The results indicated that the expressions of NLRP3 and NOX4 were significantly increased in the tubules in the T2DM model group compared with control group (Fig. 10, $P < 0.01$). Meanwhile, compared with model group, AS-IV (80 mg/kg) and Met (200 mg/kg) treatment could significantly decrease the expressions of NLRP3 and NOX4 in the tubules (Fig. 10, $P < 0.05$ or $P < 0.01$). The data suggested that the activation of NOX4 and NLRP3 inflammasome might play important roles in the progression of DN, and AS-IV

treatment could alleviate renal tubular injury via inhibiting NOX4 and NLRP3 inflammasome activation in the DN.

4. Discussion

Tubular epithelial cells damage was commonly reported as an important element in DN [19]. Meanwhile, high levels of FFAs and renal tubular damage were observed in T2DM patients and model rats [24], suggesting that excessive FFAs might play an important role of in renal tubular injury in DN. In this study, our results suggested that PA exposure could significantly exacerbate renal tubular epithelial cells damage, which were also found in the T2DM rats. However, AS-IV treatment significantly attenuated renal tubular damage in vitro and in vivo. Meanwhile, the results also indicated that NOX4 and NLRP3 inflammasome were significantly increased in PA-induced HK-2 cells and in renal tubules of T2DM rats, while AS-IV treatment significantly inhibited the expressions of NOX4 and NLRP3 inflammasome in vitro and in vivo. These data suggested that AS-IV treatment could protect against excessive FFAs-induced renal tubules damage via inhibiting the NOX4 and NLRP3 inflammasome activation.

Excessive FFAs-induced lipids deposition in tissues is one of the most important factors that induce oxidative stress and inflammation in various tissues and organs of the body [25–27]. PA is an important member of the saturated fatty acid family and closely involves in the occurrence and development of a lot of diseases in the body, such as insulin resistance and T2DM [28–30]. When the body's lipids are overloaded, the lipid balance is disrupted, leading to lipid metabolism system unable to proceed normally and cause lipotoxicity [31, 32]. It has been reported that cellular lipotoxicity contributes to obesity-related nephropathy [33]. The main saturated fatty acids, such as PA, has shown contributions to renal damage through increasing excessive ROS generation, apoptosis and endoplasmic reticulum (ER) stress [34, 35]. In our previous studies, obvious renal lipid deposition and tubules damages were found in PA-induced HK-2 cells and T2DM rats [33, 36]. In this study, we found that, with the prolongation of PA exposure, the cells viability was significantly decreased, and the apoptosis and lipids deposition were also significantly increased in HK-2 cells. However, AS-IV treatment significantly increased the cells viability, and decreased the apoptosis and lipids deposition in PA-induced HK-2 cells. And the in vivo study also suggested that AS-IV treatment could significantly attenuate the lipids deposition in tubules and ameliorate the pathological injury of renal tubules in T2DM rats. The data suggest that AS-IV has protective effect on PA-induced renal tubular damages.

At present, the potential molecular mechanisms of excessive FFA-induced renal tubular damages still remain unclear. Oxidative stress and inflammation have been reported to play important roles in the evolution of DN [37]. Oxidative stress occurs when the excessive generation of ROS overloads the ability of the organic antioxidant system and causes damage to DNA, proteins and lipid [38]. Excessive ROS generation has been characterized in DN, and impaired antioxidant defense system is also observed in obesity-associated metabolic syndrome [39–41]. In recent years, growing studies have indicated that NADPH oxidase (NOX) is an important source of ROS generation in body [42]. The NOX is composed of a membrane subunit (NOX1-5) and catalytic subunits of p47phox, p22phox, p67phox. Growing studies

confirmed that NOX4 is widely expressed in renal tubular epithelial cells, and abnormal expression of NOX4 is closely related to renal tubular damages [43, 44]. It has been reported that glycosylated albumin can induce the up-regulation of NOX4 expression, leading to fibrosis and apoptosis in NRK-52E cells, and promoting the development of DN [45]. However, it is still unknown whether NOX4 is involved in PA-induced renal tubular damages. GSH and SOD play important roles in keeping balance of oxidation and antioxidant capacity in the body, and the amount of them can also reflect the body's antioxidant capacity [46]. Previous studies showed that AS-IV significantly inhibited high glucose-induced apoptosis of HK-2 cell via increasing the antioxidant enzymes activities of GSH, SOD and CAT, and reduced the high glucose-induced ROS generation in HK-2 cells [1]. In the present study, our results suggested that PA exposure significantly increased ROS production and NOX4 expression, and decreased the GSH and SOD levels in HK-2 cells. Meanwhile, our results also indicated that the expressions of NOX4, phox22 and phox47 were significantly increased in the renal tubules in T2DM rats. Apocynin (Apo) is often used as a NOX inhibitor, which can inhibit the activity of NOX by interfering with the intracellular translocation of p47phox and p67phox [47]. The present results showed that both AS-IV and Apo treatment could significantly decrease the ROS accumulation, NOX4 expression and increase the levels of GSH and SOD in PA-induced HK-2 cells. Meanwhile, AS-IV treatment also reduced the expressions of NOX4, phox22 and phox47 in the renal tubules in T2DM rats. These data suggested that AS-IV could attenuate PA-induced ROS oxidative stress by inhibiting NOX4 expression in renal tubular epithelial cells.

Inflammation is also an important cause for renal tubules damages contributing to DN. In recent years, increasing data have characterized the diabetic renal fibrosis as a chronic inflammatory response [48]. For example, DN is accompanied by infiltration of inflammatory cells, up-regulation of inflammatory cytokines and inflammatory responses in the kidney [49]. Inhibition of inflammatory responses has been reported to have protective effect on experimental diabetic kidney disease [50]. Inflammasomes play a central role in the inflammatory response, and activation of inflammasomes can cleave the procaspase-1 to caspase-1, eventually increasing the generation of proinflammatory factors, such as IL-1β and IL-18 [15]. The NLRP3 is a core of the inflammasome, and has been reported to be involved in the progression of renal fibrosis and contribute to the pathogenesis of chronic kidney disease and DN [17]. Previous research showed that the expressions of NLRP3, caspase-1, along with the maturation of IL-1β and IL-18 were significantly increased in high glucose-induced HK-2 cells [51]. Also, it has been reported that accumulation of ROS contributes to HG-induced activation of NLRP3 inflammasome in epithelial cells [52]. In addition, studies have shown that AS-IV can inhibit NLRP3 inflammasome activation and the pro-inflammatory cytokines expression to play an anti-inflammatory effect by improving antioxidant capacity, resulting in attenuation of lipopolysaccharide-induced acute kidney injury [53–55]. Our preliminary experiments also indicated that AS-IV could significantly reduce HK-2 cells injury and apoptosis [22]. However, it is still not completely understood whether AS-IV protects against PA-induced renal tubular injury by regulating NOX4-NLPR3 inflammasome. In this work, the results showed that the expressions of NLRP3, ASC, caspase-1, and pro-inflammatory factors of IL-1β and IL-18 were significantly increased in PA-induced HK-2 cells and in renal tubules of T2DM rats. After AS-IV and Apo treatment, the expressions of NLRP3, ASC, caspase-1, IL-1β and IL-18 were significantly decreased in PA-induced HK-2 cells.

Meanwhile, the results in vivo also indicated that AS-IV and Met treatment could significantly down-regulate the expressions of NLRP3, ASC, caspase-1 and IL-1β in renal cortex of T2DM rats. The data suggested that PA exposure might mediate the inflammatory response by activating the NLRP3 inflammasome in DN. And AS-IV treatment might alleviate the PA-induced renal tubular damages through inhibiting the NLRP3 inflammasome expression.

5. Conclusion

In general, our study indicated that AS-IV treatment alleviated renal tubular epithelial cells injury both in PA-induced HK-2 cells and in renal tubules of T2DM rat, and the mechanism may be related to inhibition of NOX4 and NLRP3 inflammasome, which attenuates oxidative stress and inflammation. However, this study only provided the protective effect of AS-IV on PA-induced HK-2 cells, the effect and mechanism of high glucose and hyperlipidemia on renal tubular epithelial cells remain for further study. Nevertheless, this study provides evidence for the protective effect of AS-IV on PA-induced renal tubular epithelial cells damage. Furthermore, regulating NOX4 and NLRP3 inflammasome may be an effective strategy to improve renal tubules damage in T2DM.

Abbreviations

DN: diabetic nephropathy; T2DM: type 2 diabetes mellitus; PA: palmitic acid; AS-IV: Astragaloside IV; ROS: reactive oxygen species; NOX4: nicotinamide adenine dinucleotide phosphate (NADPH) oxidase 4; NLRP3: nod-like receptor protein 3

Declarations

Acknowledgments

Not applicable.

Authors' contributions

ZYH and SY proposed the conception; ZYH, LY, SY, DXN, HYL and ZYF designed and investigated the study analysis; ZYH, LWZ and LWP contributed to writing, reviewing and supervising the manuscript; LWP and LWZ funded the study. All authors read and approved the final manuscript.

Funding

This study was supported by grants from the National Natural Science Foundation of China (81970630); the major science and technology projects in Anhui Province (201903a07020025).

Availability of data and materials

All data and materials in the current study are included in this published article

Ethics approval and consent to participate

The animal experiments were approved by the Institutional Ethics Committee of Anhui Medical University.

Content for publication

Not applicable.

Competing interests

The authors declare no competing interests.

References

1. Wang J and Guo HM. Astragaloside IV ameliorates high glucose-induced HK-2 cell apoptosis and oxidative stress by regulating the Nrf2/ARE signaling pathway. Exp Ther Med, 2019, 17(6): 4409-4416.
2. Hovind P, Tarnow L, Rossing K*, et al.* Decreasing incidence of severe diabetic microangiopathy in type 1 diabetes. Diabetes Care, 2003, 26(4): 1258-1264.
3. Brezniceanu ML, Lau CJ, Godin N*, et al.* Reactive oxygen species promote caspase-12 expression and tubular apoptosis in diabetic nephropathy. J Am Soc Nephrol, 2010, 21(6): 943-954.
4. Spiller S, Blüher M and Hoffmann R. Plasma levels of free fatty acids correlate with type 2 diabetes mellitus. Diabetes Obes Metab, 2018, 20(11): 2661-2669.
5. Xu S, Nam SM, Kim JH*, et al.* Palmitate induces ER calcium depletion and apoptosis in mouse podocytes subsequent to mitochondrial oxidative stress. Cell Death Dis, 2015, 6(11): e1976.
6. Gao Q, Qin WS, Jia ZH*, et al.* Rhein improves renal lesion and ameliorates dyslipidemia in db/db mice with diabetic nephropathy. Planta Med, 2010, 76(1): 27-33.
7. Mahwish UN, Ponnaluri KC, Heera B*, et al.* Link between ACE I/D Gene Polymorphism and Dyslipidemia in Diabetic Nephropathy: A Case-control Study from Hyderabad, India. Indian J Nephrol, 2020, 30(2): 77-84.
8. Lim JC, Lim SK, Han HJ*, et al.* Cannabinoid receptor 1 mediates palmitic acid-induced apoptosis via endoplasmic reticulum stress in human renal proximal tubular cells. J Cell Physiol, 2010, 225(3): 654-663.
9. Huang Y, Mao Z, Zhang Z*, et al.* Connexin43 Contributes to Inflammasome Activation and Lipopolysaccharide-Initiated Acute Renal Injury via Modulation of Intracellular Oxidative Status. Antioxid Redox Signal, 2019, 31(16): 1194-1212.
10. Holterman CE, Read NC and Kennedy CR. Nox and renal disease. Clin Sci (Lond), 2015, 128(8): 465-481.
11. Krause KH. Tissue distribution and putative physiological function of NOX family NADPH oxidases. Jpn J Infect Dis, 2004, 57(5): S28-29.

12. Yao M, Gao F, Wang X*, et al.* Nox4 is involved in high glucose-induced apoptosis in renal tubular epithelial cells via Notch pathway. Mol Med Rep, 2017, 15(6): 4319-4325.
13. Zha D, Wu S, Gao P*, et al.* Telmisartan Attenuates Uric Acid-Induced Epithelial-Mesenchymal Transition in Renal Tubular Cells. Biomed Res Int, 2019, 2019: 3851718.
14. Yi H, Peng R, Zhang LY*, et al.* LincRNA-Gm4419 knockdown ameliorates NF-κB/NLRP3 inflammasome-mediated inflammation in diabetic nephropathy. Cell Death Dis, 2017, 8(2): e2583.
15. Mamik MK and Power C. Inflammasomes in neurological diseases: emerging pathogenic and therapeutic concepts. Brain, 2017, 140(9): 2273-2285.
16. Kimura T, Isaka Y and Yoshimori T. Autophagy and kidney inflammation. Autophagy, 2017, 13(6): 997-1003.
17. Komada T and Muruve DA. The role of inflammasomes in kidney disease. Nat Rev Nephrol, 2019, 15(8): 501-520.
18. Wang M, Yang L, Yang J*, et al.* Shen Shuai IIRecipe attenuates renal injury and fibrosis in chronic kidney disease by regulating NLRP3 inflammasome and Sirt1/Smad3 deacetylation pathway. BMC Complement Altern Med, 2019, 19(1): 107.
19. Song S, Qiu D, Luo F*, et al.* Knockdown of NLRP3 alleviates high glucose or TGFB1-induced EMT in human renal tubular cells. J Mol Endocrinol, 2018, 61(3): 101-113.
20. Yao Y, Hu X, Feng X*, et al.* Dexmedetomidine alleviates lipopolysaccharide-induced acute kidney injury by inhibiting the NLRP3 inflammasome activation via regulating the TLR4/NOX4/NF-κB pathway. J Cell Biochem, 2019, 120(10): 18509-18523.
21. Song W, Wei L, Du Y*, et al.* Protective effect of ginsenoside metabolite compound K against diabetic nephropathy by inhibiting NLRP3 inflammasome activation and NF-κB/p38 signaling pathway in high-fat diet/streptozotocin-induced diabetic mice. Int Immunopharmacol, 2018, 63: 227-238.
22. Chen Q, Su Y, Ju Y*, et al.* Astragalosides IV protected the renal tubular epithelial cells from free fatty acids-induced injury by reducing oxidative stress and apoptosis. Biomed Pharmacother, 2018, 108: 679-686.
23. Li L, Hou X, Xu R*, et al.* Research review on the pharmacological effects of astragaloside IV. Fundam Clin Pharmacol, 2017, 31(1): 17-36.
24. Su LQ, Wang YD and Chi HY. Effect of curcumin on glucose and lipid metabolism, FFAs and TNF-α in serum of type 2 diabetes mellitus rat models. Saudi J Biol Sci, 2017, 24(8): 1776-1780.
25. Ly LD, Xu S, Choi SK*, et al.* Oxidative stress and calcium dysregulation by palmitate in type 2 diabetes. Exp Mol Med, 2017, 49(2): e291.
26. Su H, Li Y, Hu D*, et al.* Procyanidin B2 ameliorates free fatty acids-induced hepatic steatosis through regulating TFEB-mediated lysosomal pathway and redox state. Free Radic Biol Med, 2018, 126: 269-286.
27. Jiao P, Ma J, Feng B*, et al.* FFA-induced adipocyte inflammation and insulin resistance: involvement of ER stress and IKKβ pathways. Obesity (Silver Spring), 2011, 19(3): 483-491.

28. Hu X, Ge X, Liang W*, et al.* Effects of saturated palmitic acid and omega-3 polyunsaturated fatty acids on Sertoli cell apoptosis. Syst Biol Reprod Med, 2018, 64(5): 368-380.
29. Zhang Q, Kong X, Yuan H*, et al.* Mangiferin Improved Palmitate-Induced-Insulin Resistance by Promoting Free Fatty Acid Metabolism in HepG2 and C2C12 Cells via PPARα: Mangiferin Improved Insulin Resistance. J Diabetes Res, 2019, 2019: 2052675.
30. Lytrivi M, Castell AL, Poitout V*, et al.* Recent Insights Into Mechanisms of β-Cell Lipo- and Glucolipotoxicity in Type 2 Diabetes. J Mol Biol, 2020, 432(5): 1514-1534.
31. Oh YS, Bae GD, Baek DJ*, et al.* Fatty Acid-Induced Lipotoxicity in Pancreatic Beta-Cells During Development of Type 2 Diabetes. Front Endocrinol (Lausanne), 2018, 9: 384.
32. Chen Q, Liu M, Yu H*, et al.* Scutellaria baicalensis regulates FFA metabolism to ameliorate NAFLD through the AMPK-mediated SREBP signaling pathway. J Nat Med, 2018, 72(3): 655-666.
33. Chen Y, He L, Yang Y*, et al.* The inhibition of Nrf2 accelerates renal lipid deposition through suppressing the ACSL1 expression in obesity-related nephropathy. Ren Fail, 2019, 41(1): 821-831.
34. Cobbs A, Chen X, Zhang Y*, et al.* Saturated fatty acid stimulates production of extracellular vesicles by renal tubular epithelial cells. Mol Cell Biochem, 2019, 458(1-2): 113-124.
35. Lee E, Choi J and Lee HS. Palmitate induces mitochondrial superoxide generation and activates AMPK in podocytes. J Cell Physiol, 2017, 232(12): 3209-3217.
36. Ju Y, Su Y, Chen Q*, et al.* Protective effects of Astragaloside IV on endoplasmic reticulum stress-induced renal tubular epithelial cells apoptosis in type 2 diabetic nephropathy rats. Biomed Pharmacother, 2019, 109: 84-92.
37. Al Hroob AM, Abukhalil MH, Alghonmeen RD*, et al.* Ginger alleviates hyperglycemia-induced oxidative stress, inflammation and apoptosis and protects rats against diabetic nephropathy. Biomed Pharmacother, 2018, 106: 381-389.
38. Hou Y, Shi Y, Han B*, et al.* The antioxidant peptide SS31 prevents oxidative stress, downregulates CD36 and improves renal function in diabetic nephropathy. Nephrol Dial Transplant, 2018, 33(11): 1908-1918.
39. Ooi DJ, Chan KW, Sarega N*, et al.* Bioprospecting the Curculigoside-Cinnamic Acid-Rich Fraction from Molineria latifolia Rhizome as a Potential Antioxidant Therapeutic Agent. Molecules, 2016, 21(6).
40. Furukawa S, Fujita T, Shimabukuro M*, et al.* Increased oxidative stress in obesity and its impact on metabolic syndrome. J Clin Invest, 2004, 114(12): 1752-1761.
41. Xie C, Wu W, Tang A*, et al.* lncRNA GAS5/miR-452-5p Reduces Oxidative Stress and Pyroptosis of High-Glucose-Stimulated Renal Tubular Cells. Diabetes Metab Syndr Obes, 2019, 12: 2609-2617.
42. Shen X, Dong X, Han Y*, et al.* Ginsenoside Rg1 ameliorates glomerular fibrosis during kidney aging by inhibiting NOX4 and NLRP3 inflammasome activation in SAMP8 mice. Int Immunopharmacol, 2020, 82: 106339.
43. Cho S, Yu SL, Kang J*, et al.* NADPH oxidase 4 mediates TGF-β1/Smad signaling pathway induced acute kidney injury in hypoxia. PLoS One, 2019, 14(7): e0219483.

44. Hu F, Xue M, Li Y*, et al.* Early Growth Response 1 (Egr1) Is a Transcriptional Activator of NOX4 in Oxidative Stress of Diabetic Kidney Disease. J Diabetes Res, 2018, 2018: 3405695.
45. Qi W, Niu J, Qin Q*, et al.* Glycated albumin triggers fibrosis and apoptosis via an NADPH oxidase/Nox4-MAPK pathway-dependent mechanism in renal proximal tubular cells. Mol Cell Endocrinol, 2015, 405: 74-83.
46. Nair A and Nair BJ. Comparative analysis of the oxidative stress and antioxidant status in type II diabetics and nondiabetics: A biochemical study. J Oral Maxillofac Pathol, 2017, 21(3): 394-401.
47. Stolk J, Hiltermann TJ, Dijkman JH*, et al.* Characteristics of the inhibition of NADPH oxidase activation in neutrophils by apocynin, a methoxy-substituted catechol. Am J Respir Cell Mol Biol, 1994, 11(1): 95-102.
48. Navarro-González JF, Mora-Fernández C, Muros de Fuentes M*, et al.* Inflammatory molecules and pathways in the pathogenesis of diabetic nephropathy. Nat Rev Nephrol, 2011, 7(6): 327-340.
49. Navarro-González JF and Mora-Fernández C. The role of inflammatory cytokines in diabetic nephropathy. J Am Soc Nephrol, 2008, 19(3): 433-442.
50. Lim AK, Ma FY, Nikolic-Paterson DJ*, et al.* Antibody blockade of c-fms suppresses the progression of inflammation and injury in early diabetic nephropathy in obese db/db mice. Diabetologia, 2009, 52(8): 1669-1679.
51. Chen K, Zhang J, Zhang W*, et al.* ATP-P2X4 signaling mediates NLRP3 inflammasome activation: a novel pathway of diabetic nephropathy. Int J Biochem Cell Biol, 2013, 45(5): 932-943.
52. Chen Y, Wang L, Pitzer AL*, et al.* Contribution of redox-dependent activation of endothelial Nlrp3 inflammasomes to hyperglycemia-induced endothelial dysfunction. J Mol Med (Berl), 2016, 94(12): 1335-1347.
53. Qu X, Gao H, Tao L*, et al.* Astragaloside IV protects against cisplatin-induced liver and kidney injury via autophagy-mediated inhibition of NLRP3 in rats. J Toxicol Sci, 2019, 44(3): 167-175.
54. Xin Y, Li G, Liu H*, et al.* AS-IV protects against kidney IRI through inhibition of NF-κB activity and PUMA upregulation. Int J Clin Exp Med, 2015, 8(10): 18293-18301.
55. Leng B, Zhang Y, Liu X*, et al.* Astragaloside IV Suppresses High Glucose-Induced NLRP3 Inflammasome Activation by Inhibiting TLR4/NF-κB and CaSR. Mediators Inflamm, 2019, 2019: 1082497.

Figures

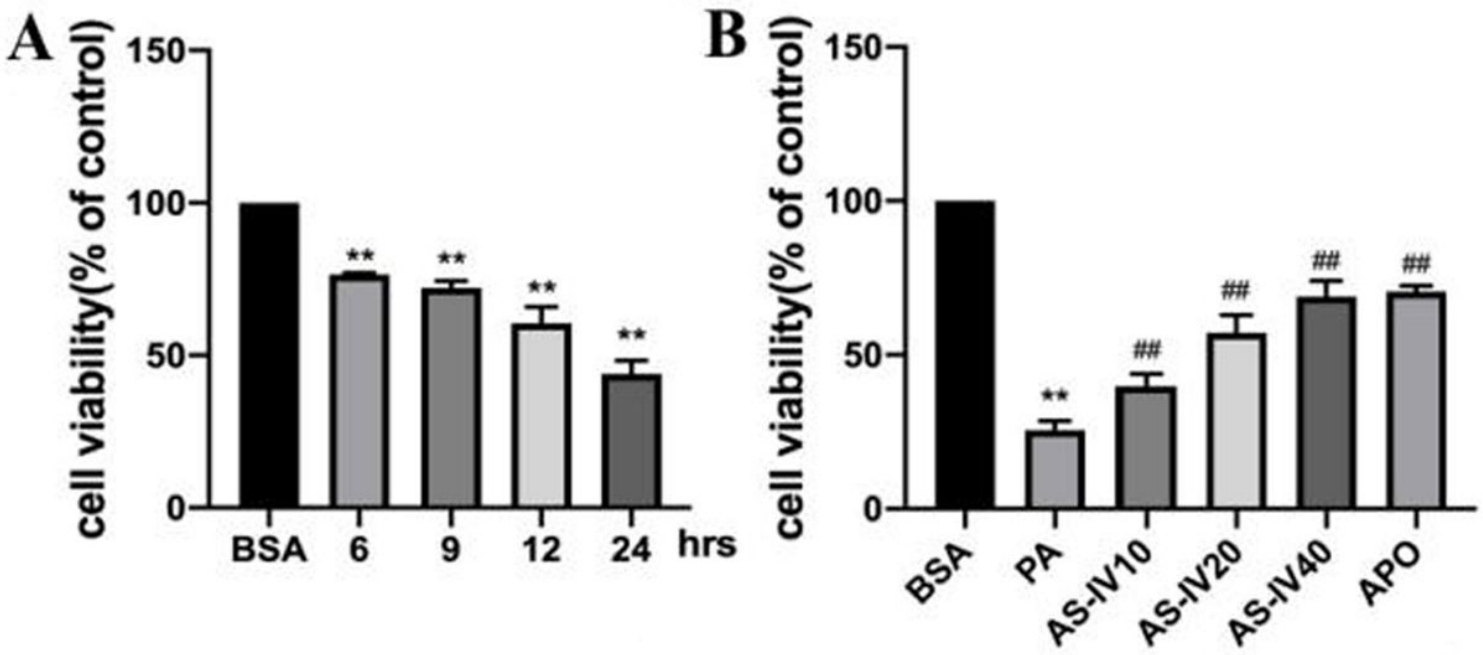

Figure 1

Effect AS-IV treatment on cell viability in PA-induced HK-2 cells (CCK-8). (A) The effect of PA exposure for different time on cell viability in HK-2 cells. (B) The effect of AS-IV treatment on cell viability in PA-induced HK-2 cells. Bars are represented as the means ± SD, n=3. **P<0.01 versus the BSA control group; ##P<0.01 versus the PA group.

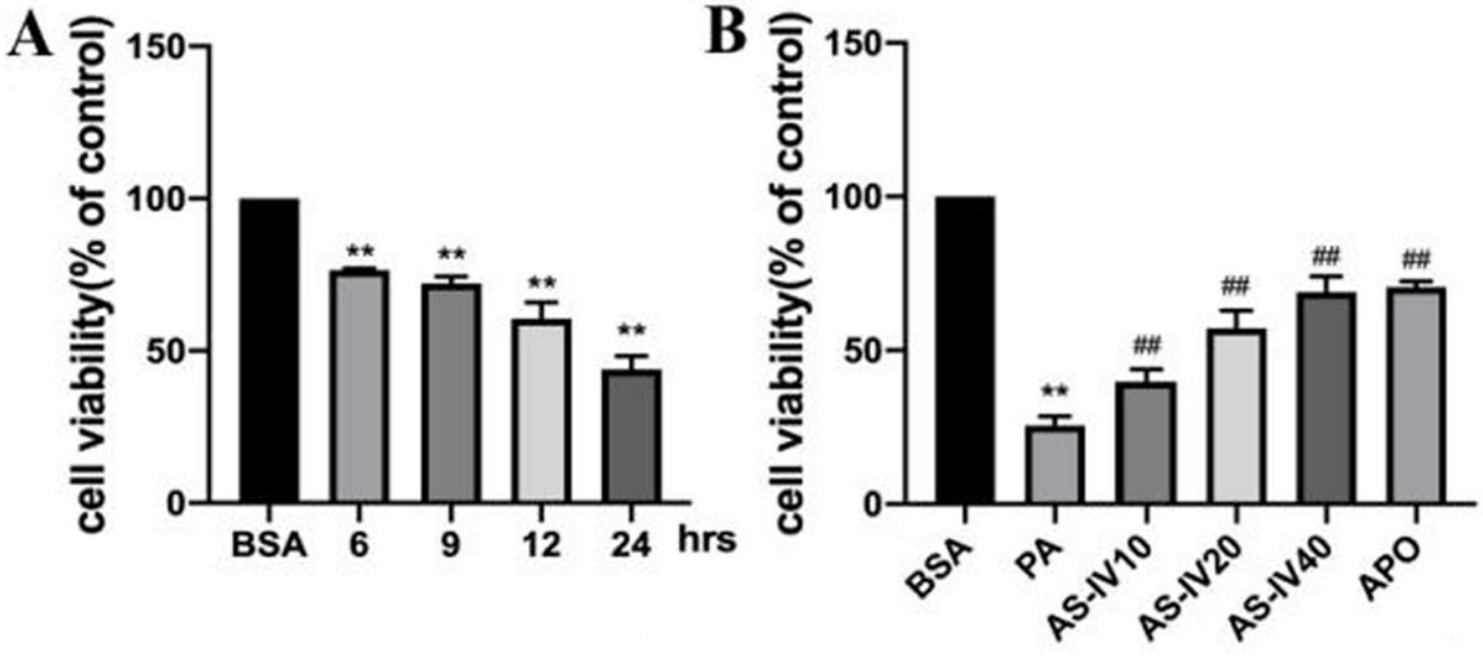

Figure 1

Effect AS-IV treatment on cell viability in PA-induced HK-2 cells (CCK-8). (A) The effect of PA exposure for different time on cell viability in HK-2 cells. (B) The effect of AS-IV treatment on cell viability in PA-induced

HK-2 cells. Bars are represented as the means ± SD, n=3. **P<0.01 versus the BSA control group; ##P<0.01 versus the PA group.

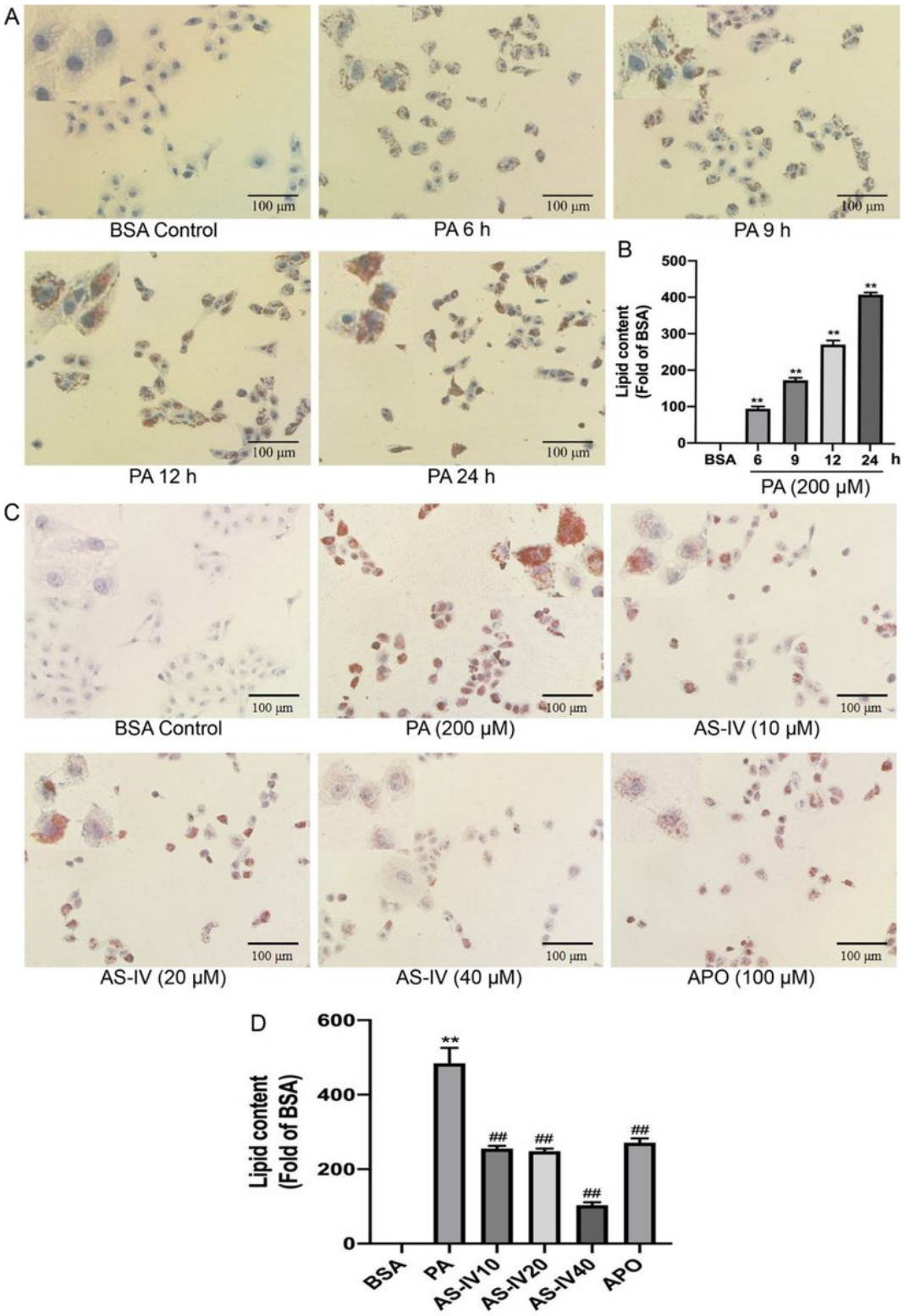

Figure 2

Effect of AS-IV treatment on lipid deposition in PA-induced HK-2 cells (Oil Red O Staining, 200×). (A) The effect of PA exposure different time on lipid deposition in HK-2 cells. (C) The effect of AS-IV treatment on

lipid deposition in PA-induced HK-2 cells. (B&D) Quantitative analysis of the results. Bars are represented as the means ± SD, n=3. **P<0.01 versus the BSA control group; ##P<0.01 versus the PA group.

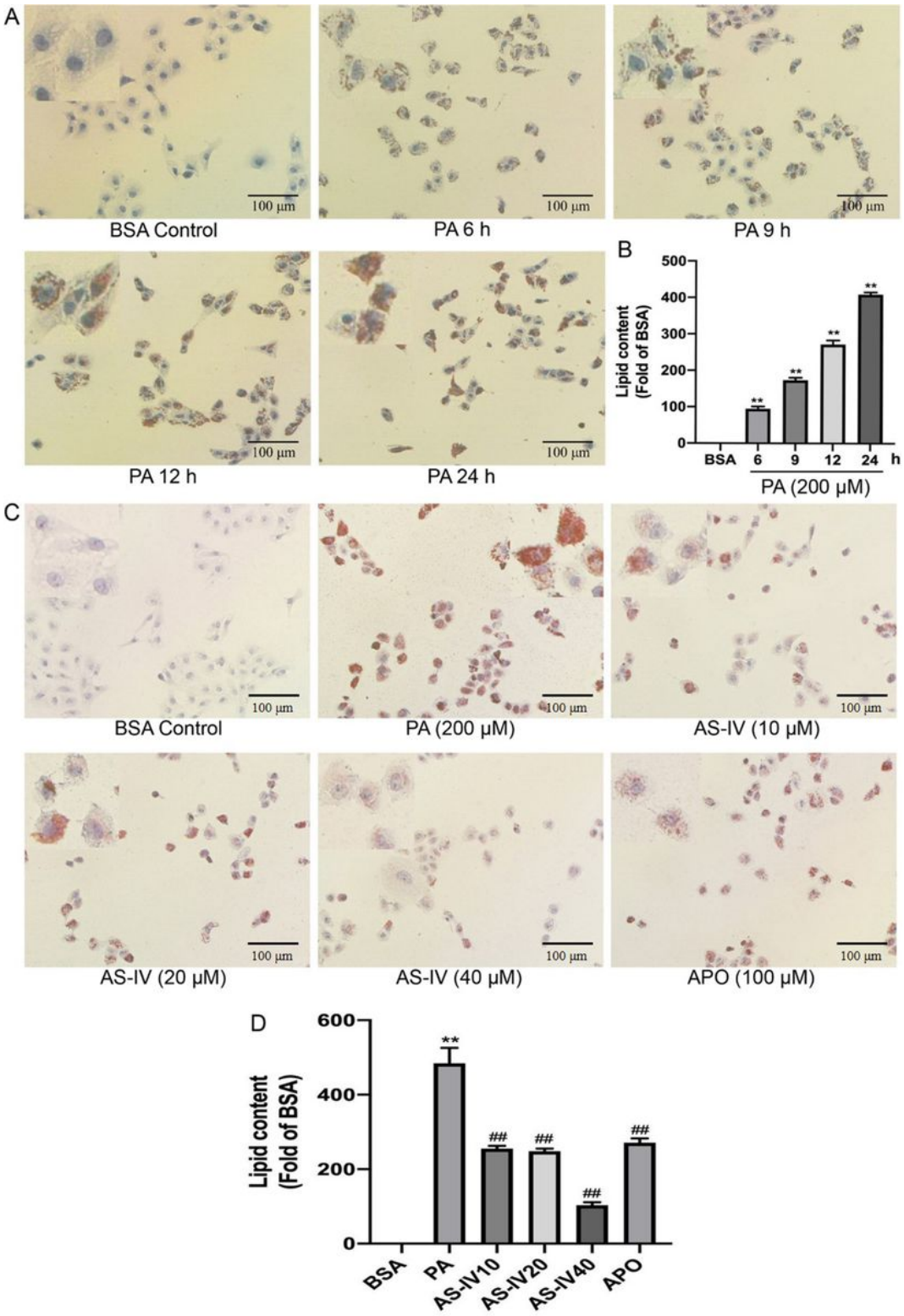

Figure 2

Effect of AS-IV treatment on lipid deposition in PA-induced HK-2 cells (Oil Red O Staining, 200×). (A) The effect of PA exposure different time on lipid deposition in HK-2 cells. (C) The effect of AS-IV treatment on

lipid deposition in PA-induced HK-2 cells. (B&D) Quantitative analysis of the results. Bars are represented as the means ± SD, n=3. **P<0.01 versus the BSA control group; ##P<0.01 versus the PA group.

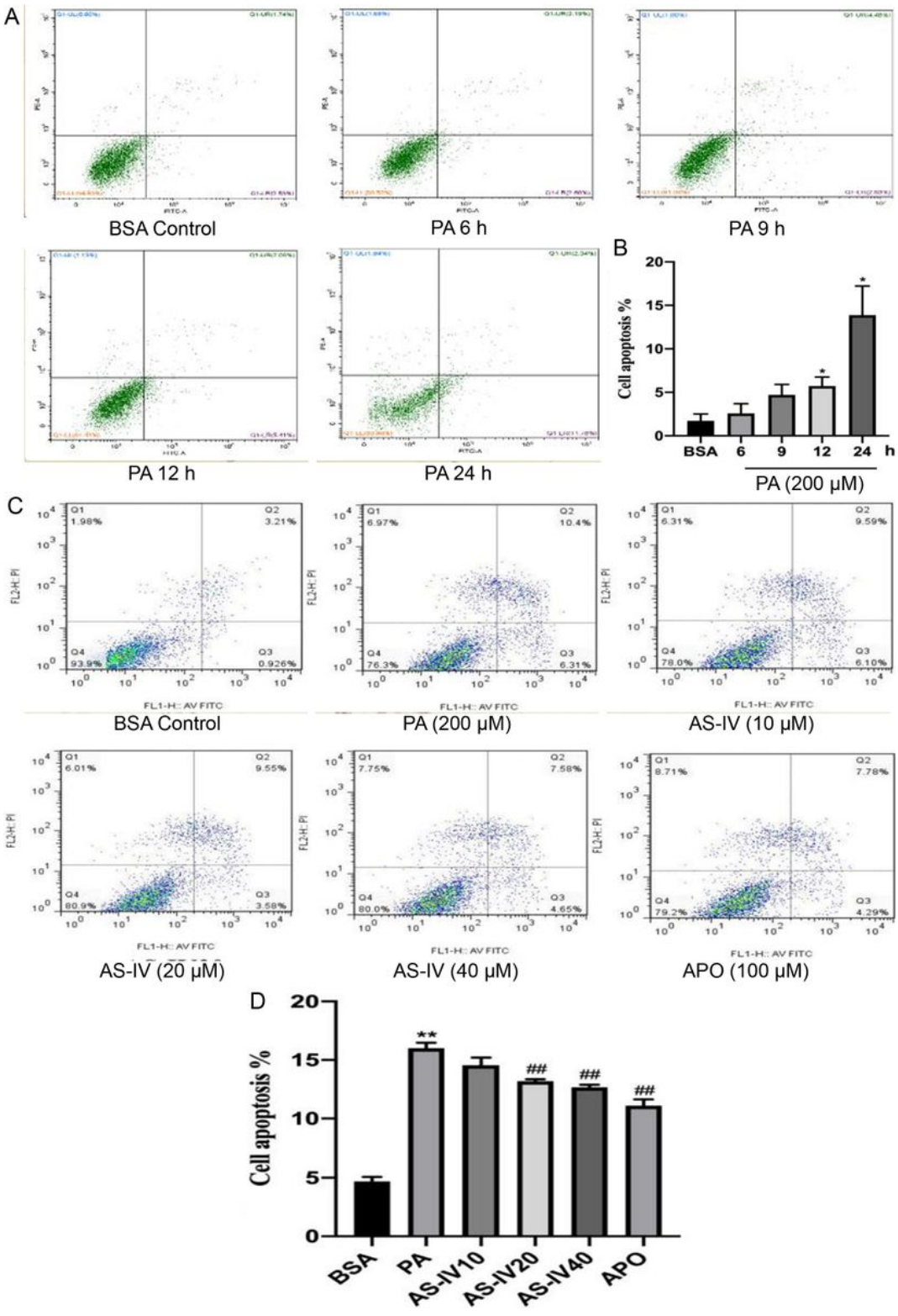

Figure 3

Effect of AS-IV treatment on apoptosis in PA-induced HK-2 cells (flow cytometry). (A) The effect of PA exposure different time on apoptosis in HK-2 cells. (C) The effect of AS-IV treatment on apoptosis in PA-induced HK-2 cells. (B&D) The apoptotic HK-2 cells were quantitatively analyzed by Graph Pad Prism.

Bars are represented as the means ± SD, n=3. *P<0.05, **P<0.01 versus the BSA control group; ##P<0.01 versus the PA group.

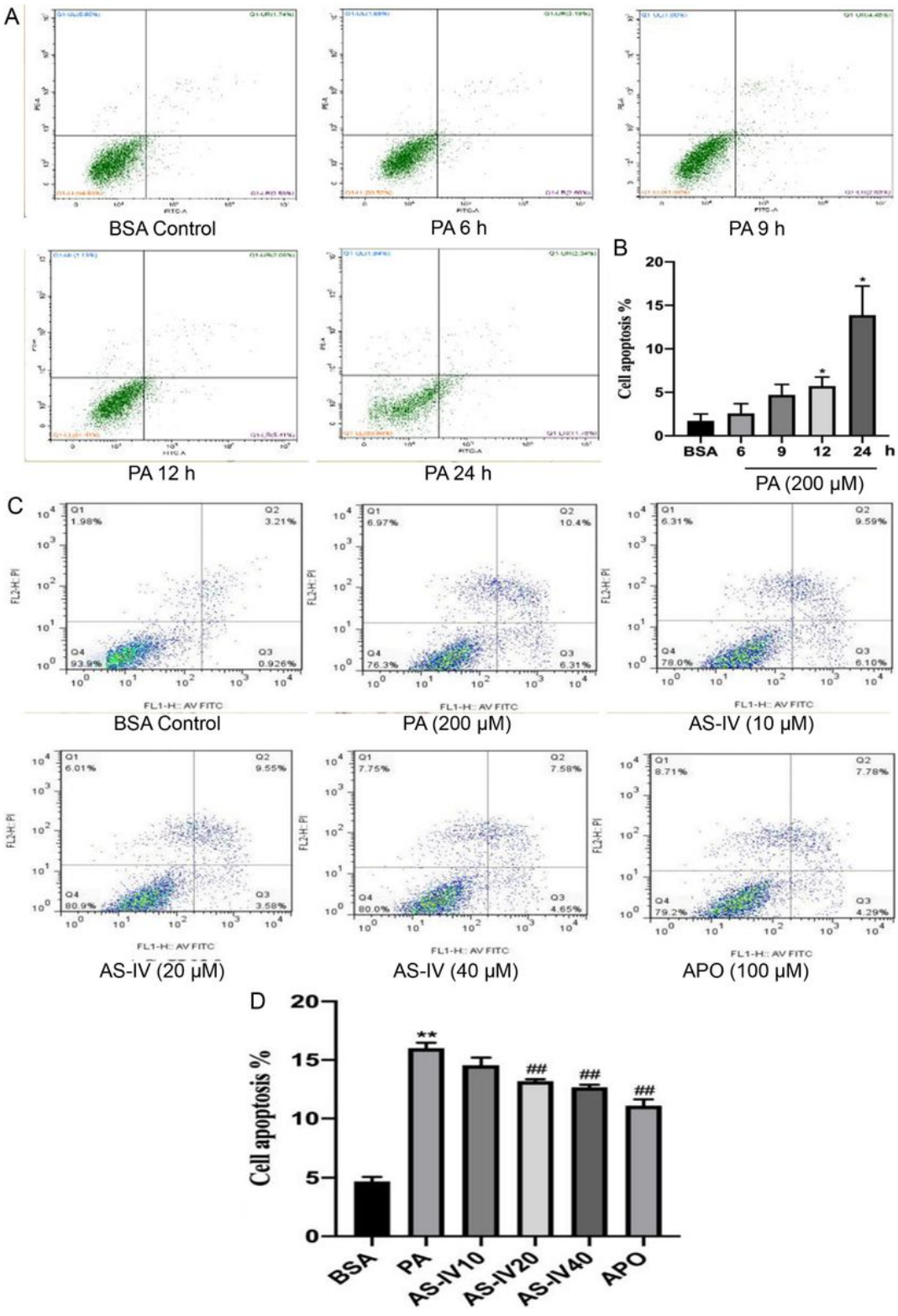

Figure 3

Effect of AS-IV treatment on apoptosis in PA-induced HK-2 cells (flow cytometry). (A) The effect of PA exposure different time on apoptosis in HK-2 cells. (C) The effect of AS-IV treatment on apoptosis in PA-induced HK-2 cells. (B&D) The apoptotic HK-2 cells were quantitatively analyzed by Graph Pad Prism.

Bars are represented as the means ± SD, n=3. *P<0.05, **P<0.01 versus the BSA control group; ##P<0.01 versus the PA group.

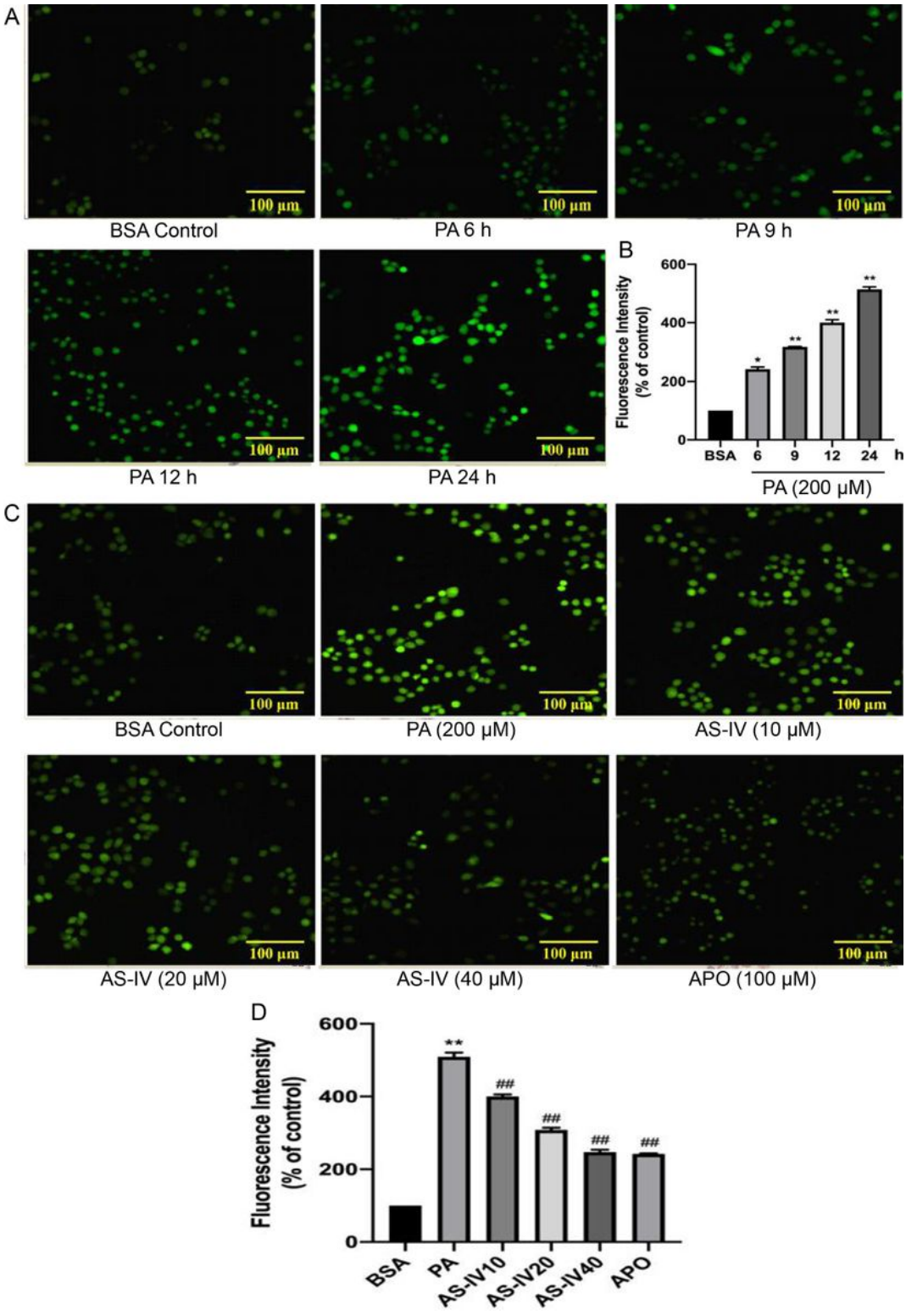

Figure 4

Effect of AS-IV treatment on ROS accumulation in PA-induced HK-2 cells (H2DCFDA staining, 200×). (A) The effect of PA exposure different time on ROS accumulation in HK-2 cells. (C) The effect of AS-IV treatment on ROS accumulation in PA-induced HK-2 cells. (B&D) Fluorescence intensity was analyzed to

indicate ROS accumulation. Bars are represented as the means ± SD, n=3. *P<0.05, **P<0.01 versus the BSA control group; ##P<0.01 versus the PA group.

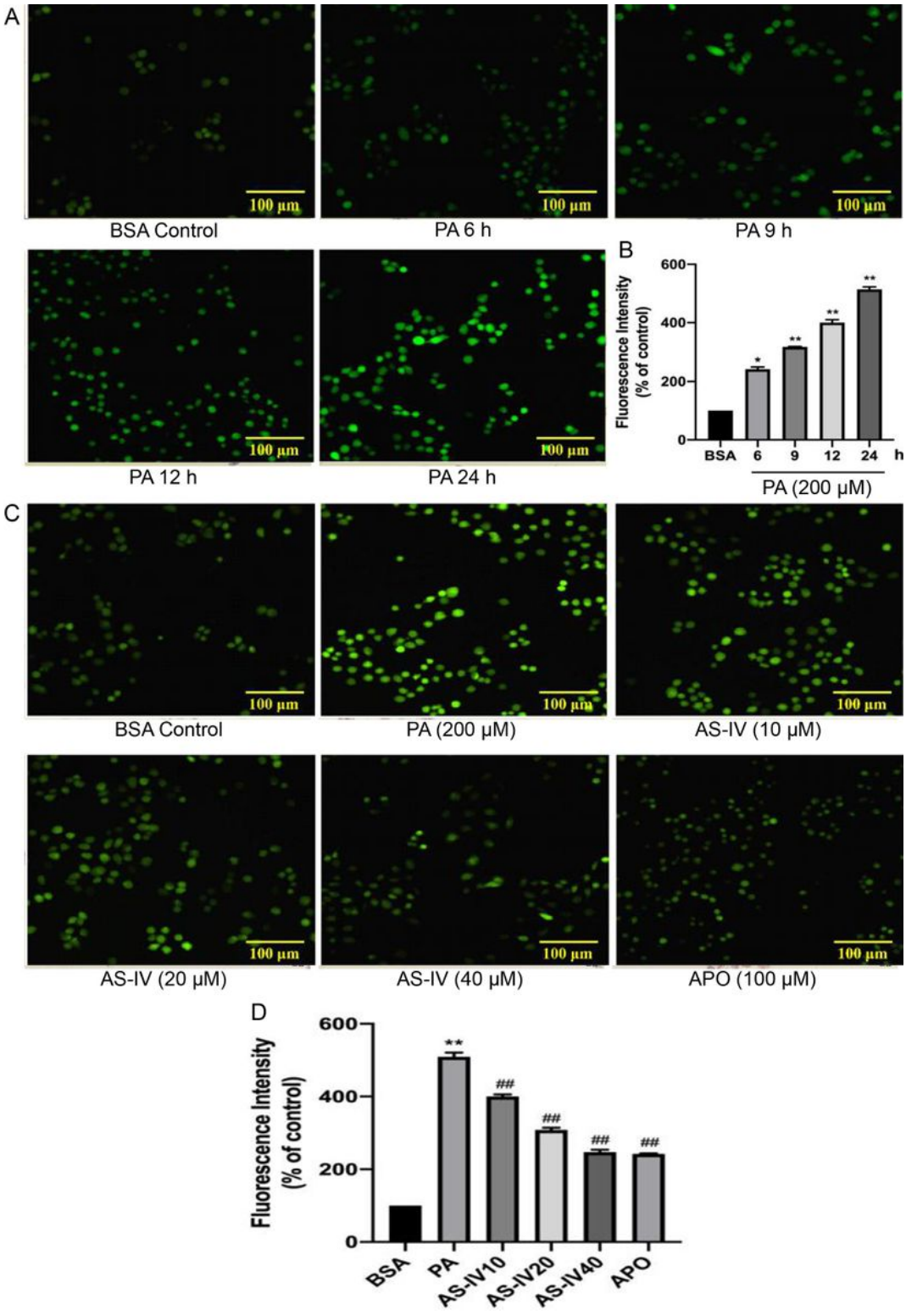

Figure 4

Effect of AS-IV treatment on ROS accumulation in PA-induced HK-2 cells (H2DCFDA staining, 200×). (A) The effect of PA exposure different time on ROS accumulation in HK-2 cells. (C) The effect of AS-IV treatment on ROS accumulation in PA-induced HK-2 cells. (B&D) Fluorescence intensity was analyzed to

indicate ROS accumulation. Bars are represented as the means ± SD, n=3. *P<0.05, **P<0.01 versus the BSA control group; ##P<0.01 versus the PA group.

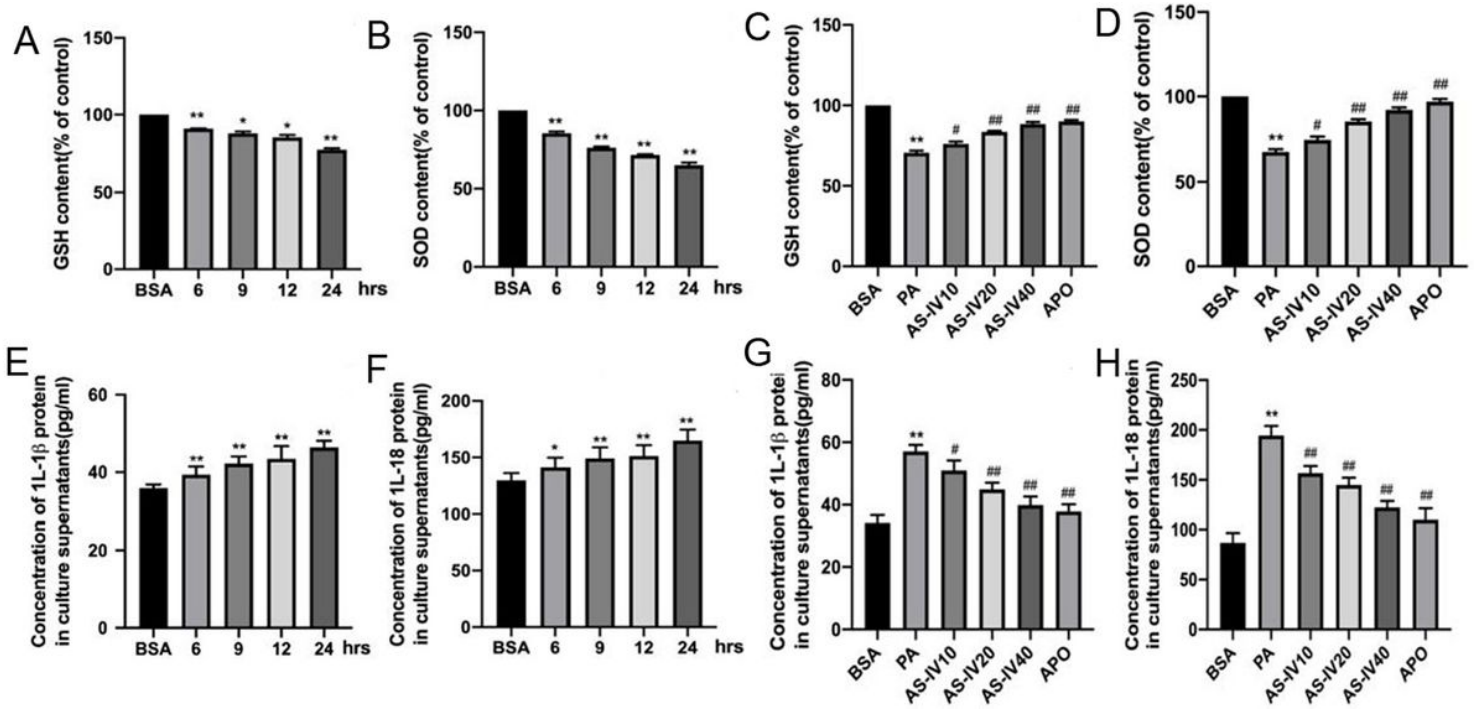

Figure 5

Effect of AS-IV treatment on the expressions of GSH, SOD, IL-1β and IL-18 in PA-induced HK-2 cells (ELISA). (A&B) The effect of PA exposure different time on expressions of GSH and SOD in HK-2 cells. (C&D) The effect of AS-IV treatment on expressions of GSH and SOD in PA-induced HK-2 cells. (E&F) The effect of PA exposure different time on expressions of IL-1β and IL-18 in supernatant. (G&H) The effect of AS-IV treatment on expressions of IL-1β and IL-18 in supernatant of PA-induced HK-2 cells. Bars are represented as the means ± SD, n=3. *P<0.05, **P<0.01 versus the BSA control group; #P<0.05, ##P<0.01 versus the PA group.

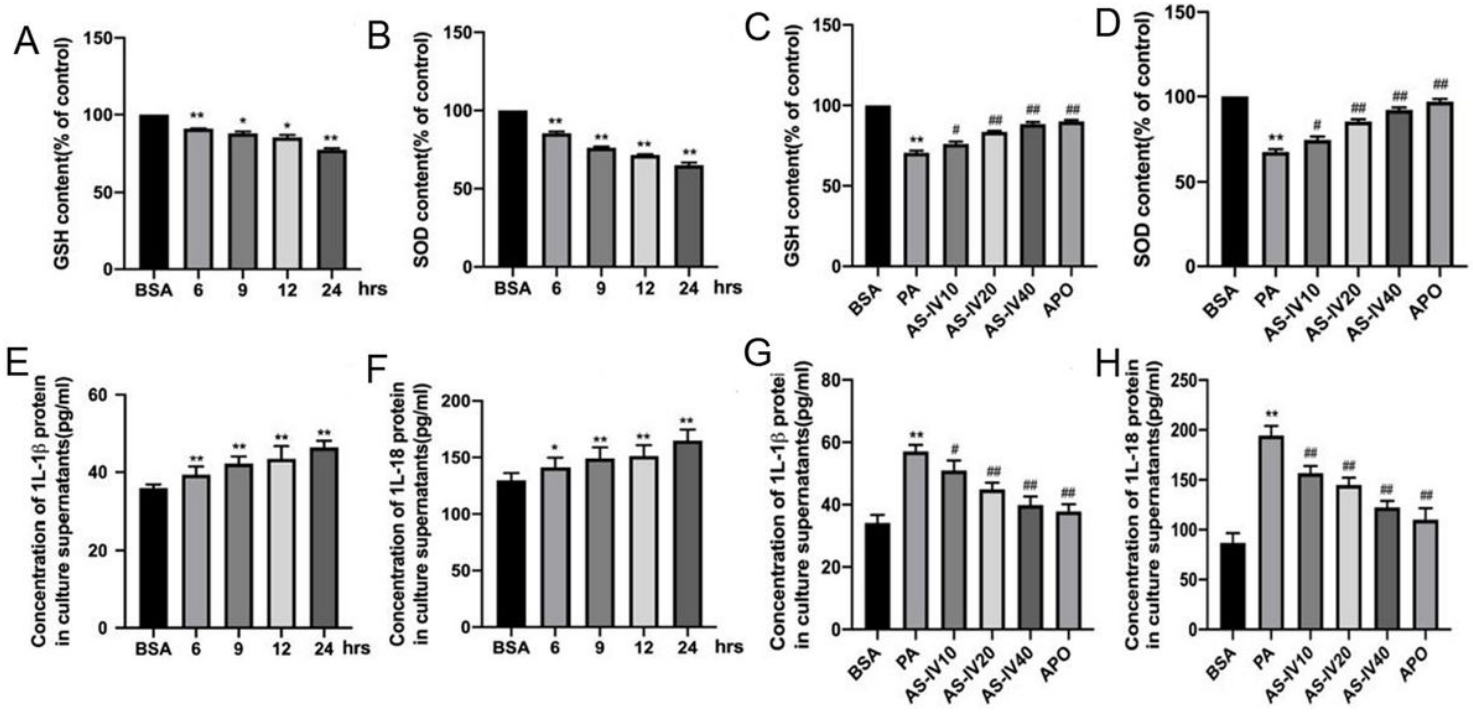

Figure 5

Effect of AS-IV treatment on the expressions of GSH, SOD, IL-1β and IL-18 in PA-induced HK-2 cells (ELISA). (A&B) The effect of PA exposure different time on expressions of GSH and SOD in HK-2 cells. (C&D) The effect of AS-IV treatment on expressions of GSH and SOD in PA-induced HK-2 cells. (E&F) The effect of PA exposure different time on expressions of IL-1β and IL-18 in supernatant. (G&H) The effect of AS-IV treatment on expressions of IL-1β and IL-18 in supernatant of PA-induced HK-2 cells. Bars are represented as the means ± SD, n=3. *P<0.05, **P<0.01 versus the BSA control group; #P<0.05, ##P<0.01 versus the PA group.

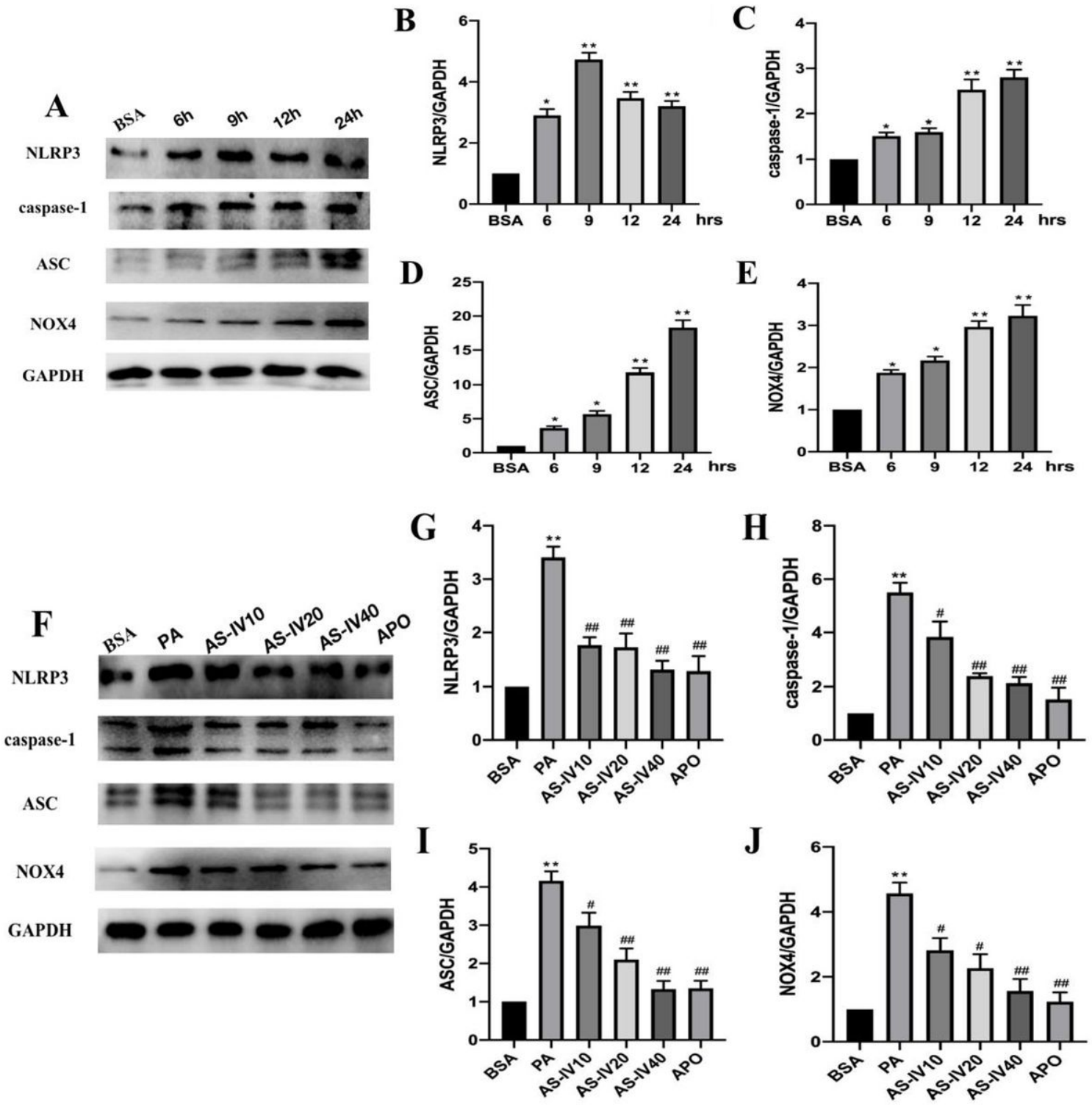

Figure 6

Effect of AS-IV treatment on expression of NLRP3, ASC, caspase-1 and NOX4 in PA-induced HK-2 cells (Western blot). (A) Results of PA stimulation for different times on expressions of NLRP3, ASC, caspase-1 and NOX4 in HK-2 cells. (B-E) The relative expressions of NLRP3, ASC, caspase-1 and NOX4 proteins over BSA control. (F) Results of AS-IV treatment on expressions of NLRP3, ASC, caspase-1 and NOX4 in PA-induced HK-2 cells. (G-J) The effect of AS-IV treatment on relative expressions of NLRP3, ASC, caspase-1

and NOX4 proteins over BSA control. Bars are represented as the means ± SD, n=3. *P<0.05, **P<0.01 versus the BSA control group; #P<0.05, ##P<0.01 versus the PA group.

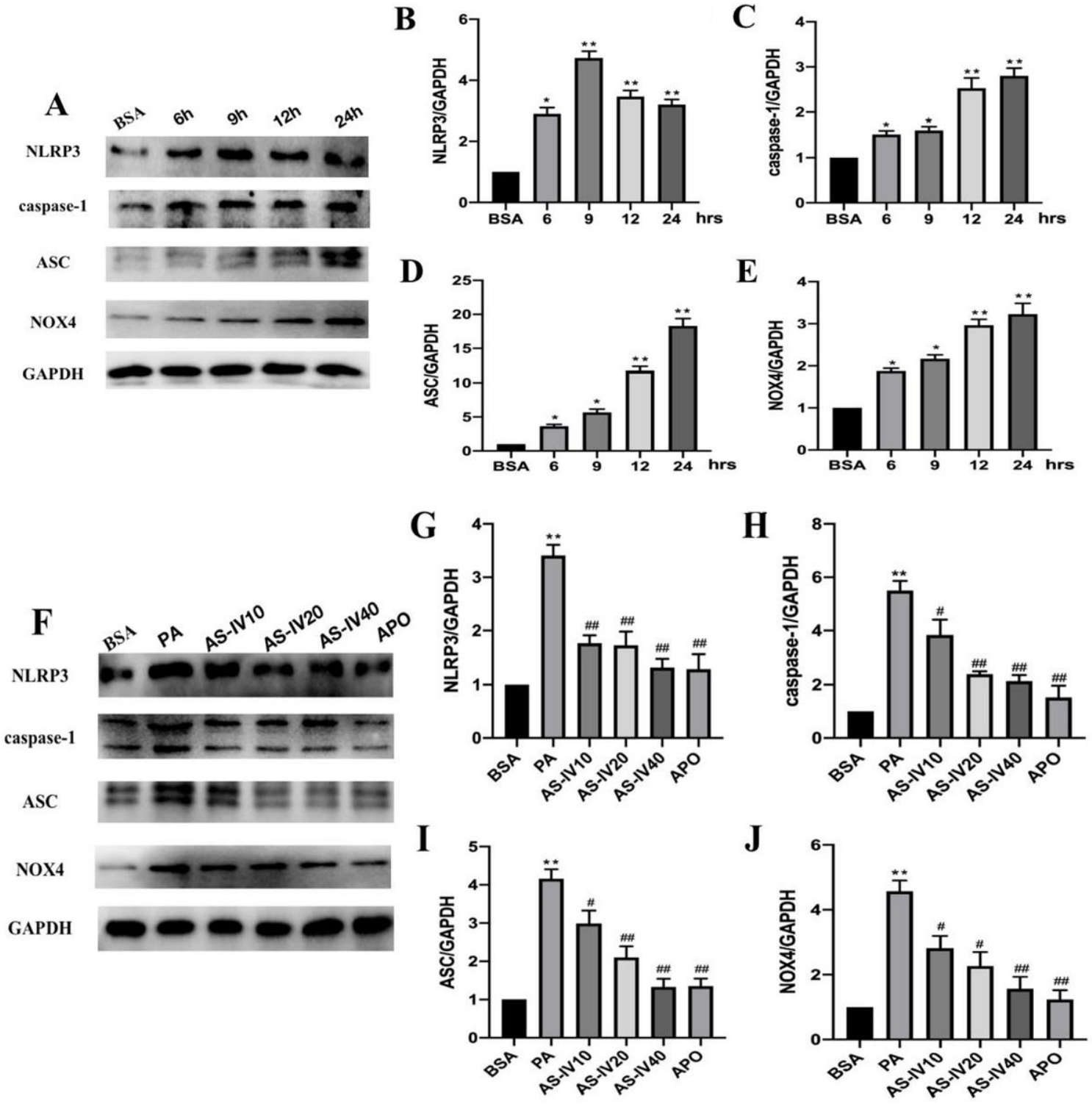

Figure 6

Effect of AS-IV treatment on expression of NLRP3, ASC, caspase-1 and NOX4 in PA-induced HK-2 cells (Western blot). (A) Results of PA stimulation for different times on expressions of NLRP3, ASC, caspase-1 and NOX4 in HK-2 cells. (B-E) The relative expressions of NLRP3, ASC, caspase-1 and NOX4 proteins over BSA control. (F) Results of AS-IV treatment on expressions of NLRP3, ASC, caspase-1 and NOX4 in PA-

induced HK-2 cells. (G-J) The effect of AS-IV treatment on relative expressions of NLRP3, ASC, caspase-1 and NOX4 proteins over BSA control. Bars are represented as the means ± SD, n=3. *P<0.05, **P<0.01 versus the BSA control group; #P<0.05, ##P<0.01 versus the PA group.

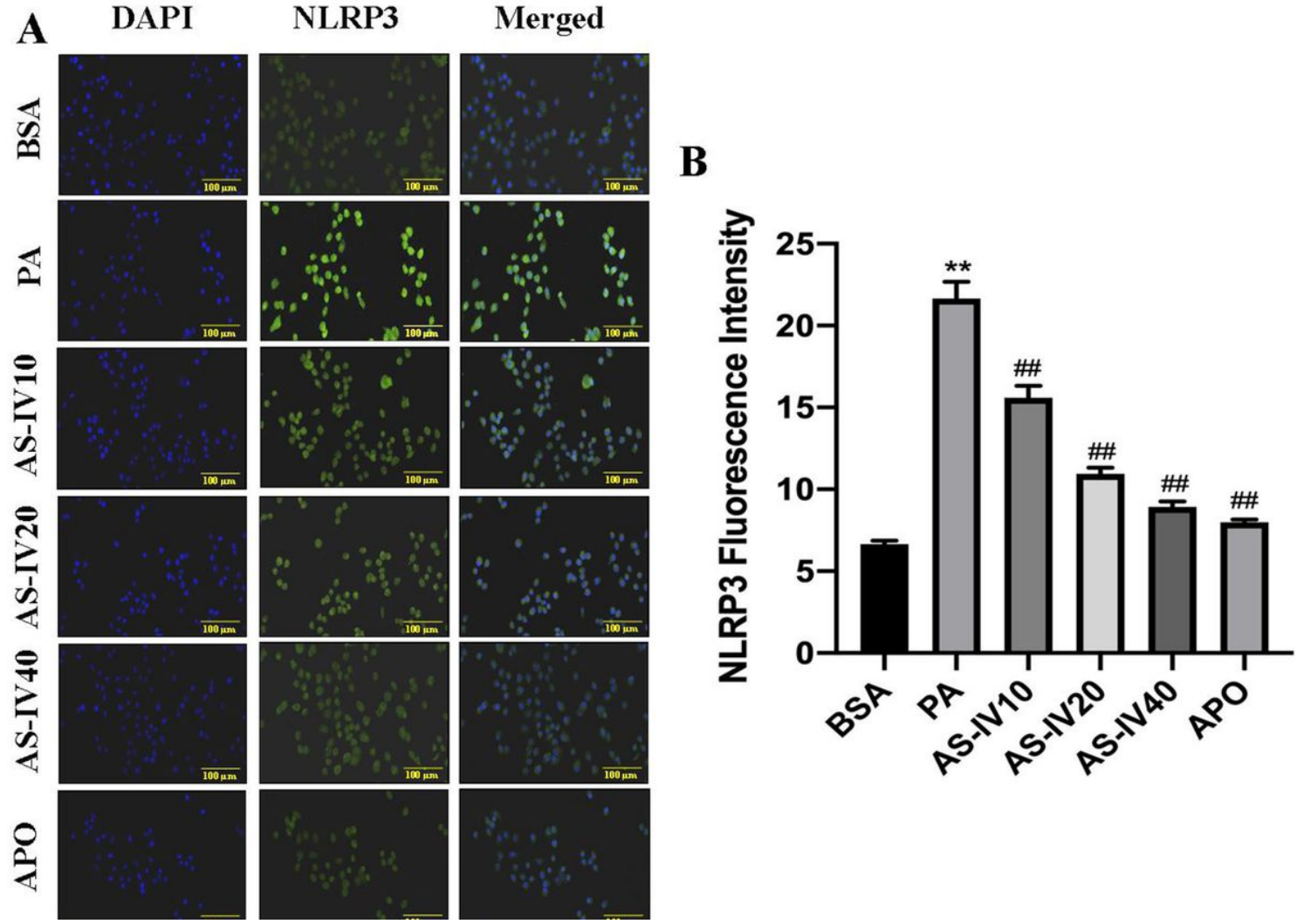

Figure 7

Effect of AS-IV treatment on expression of NLRP3 in PA-induced HK-2 cells (immunofluorescence, 200×). (A) The results of NLRP3 expression (green). (B) The relative expression of NLRP3 (fluorescence intensity). Bars are represented as the means ± SD, n = 3. **P<0.01 versus the BSA control group; ##P<0.01 versus the PA group.

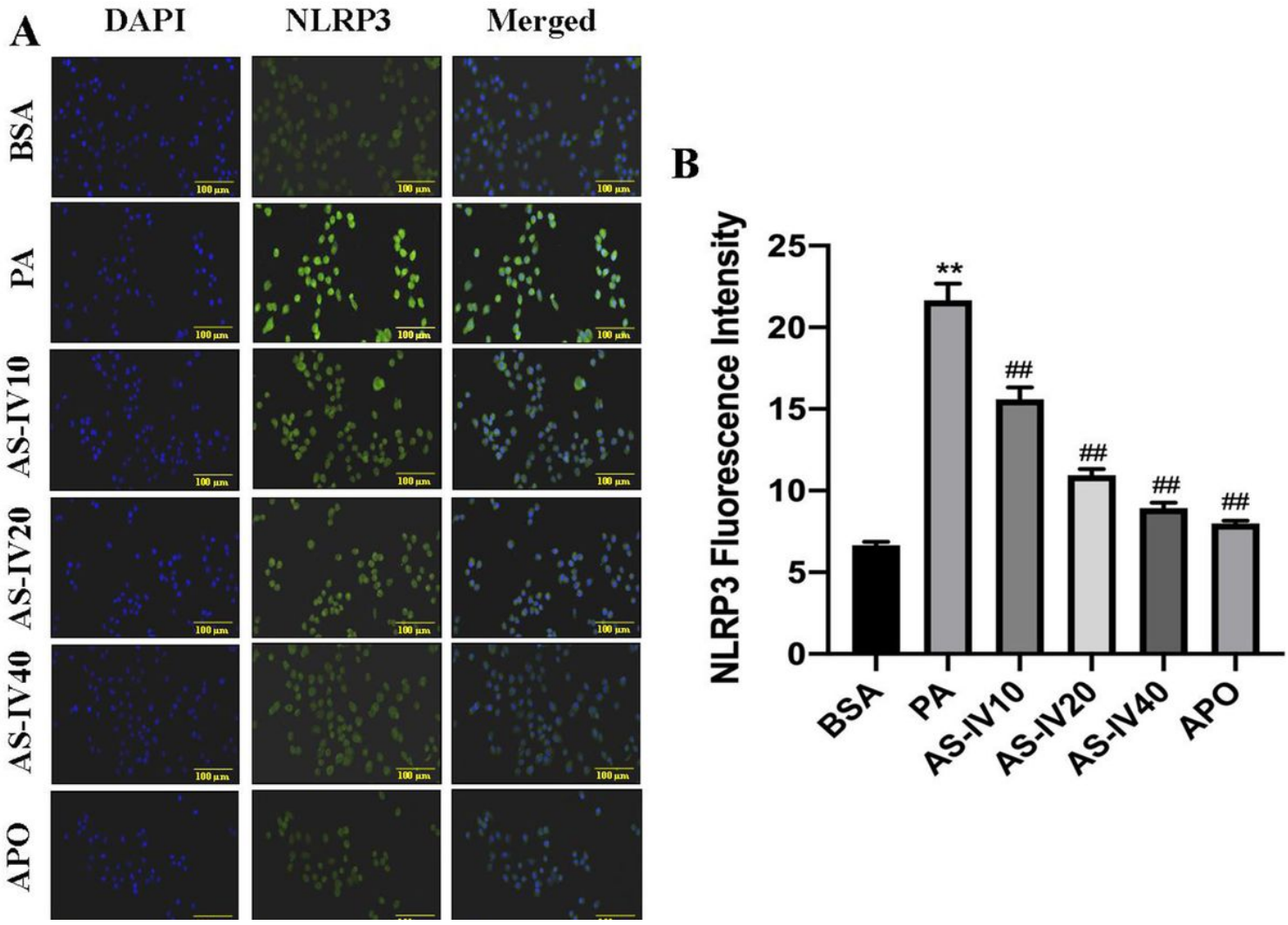

Figure 7

Effect of AS-IV treatment on expression of NLRP3 in PA-induced HK-2 cells (immunofluorescence, 200×). (A) The results of NLRP3 expression (green). (B) The relative expression of NLRP3 (fluorescence intensity). Bars are represented as the means ± SD, n = 3. **P<0.01 versus the BSA control group; ##P<0.01 versus the PA group.

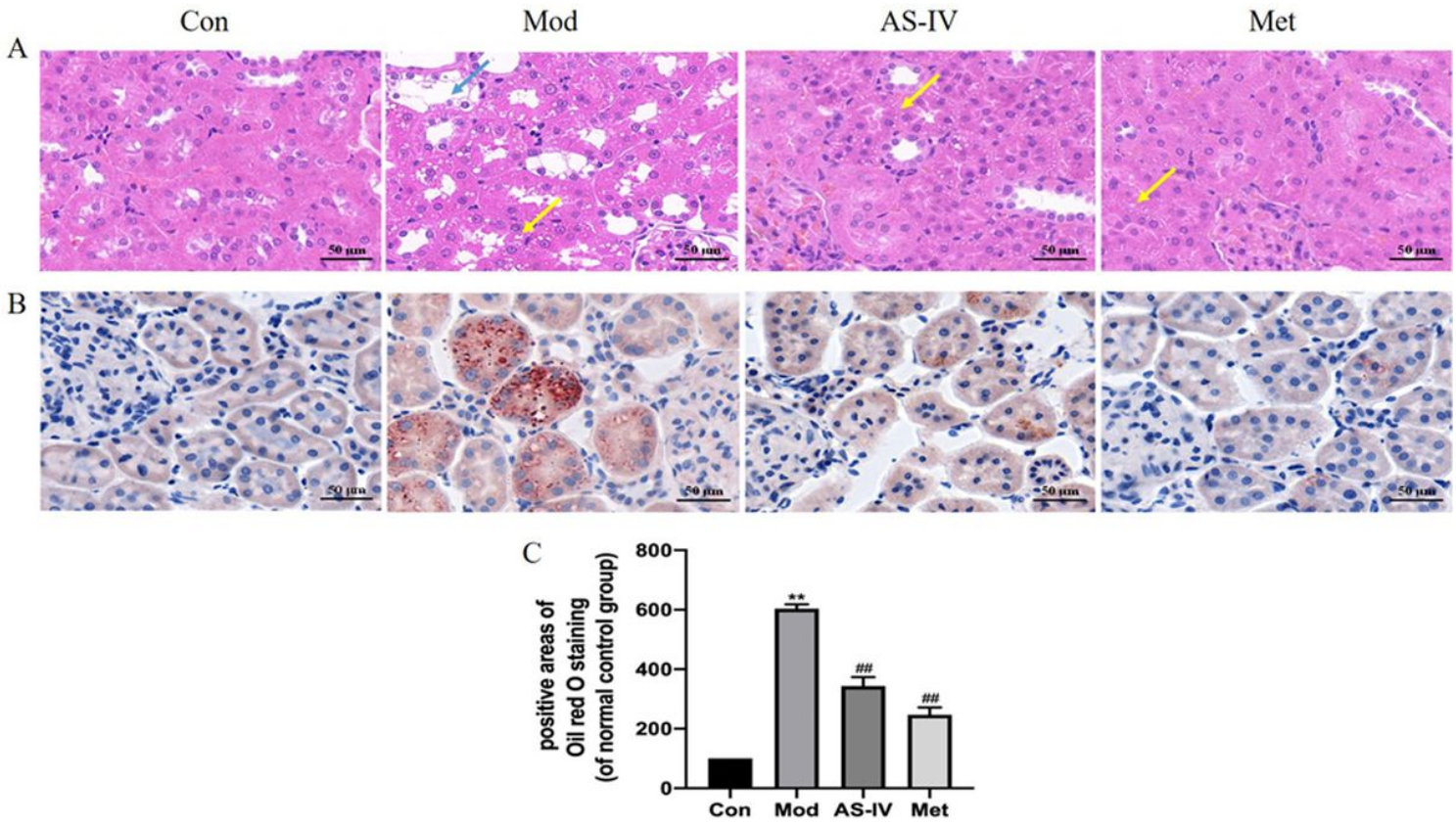

Figure 8

Effect of AS-IV treatment on renal histopathology and lipid deposition in T2DM rats. (A) The effect of AS-IV treatment on renal histopathology in T2DM rats (H&E staining, 400×). (B) The effect of AS-IV treatment on lipid deposition in T2DM rats (Oil red O staining, 400×). (C) Quantitative analysis of lipid deposition. Bars are represented as the means ± SD, n = 5. **P<0.01 compared with control group; ##P<0.01 compared with model group.

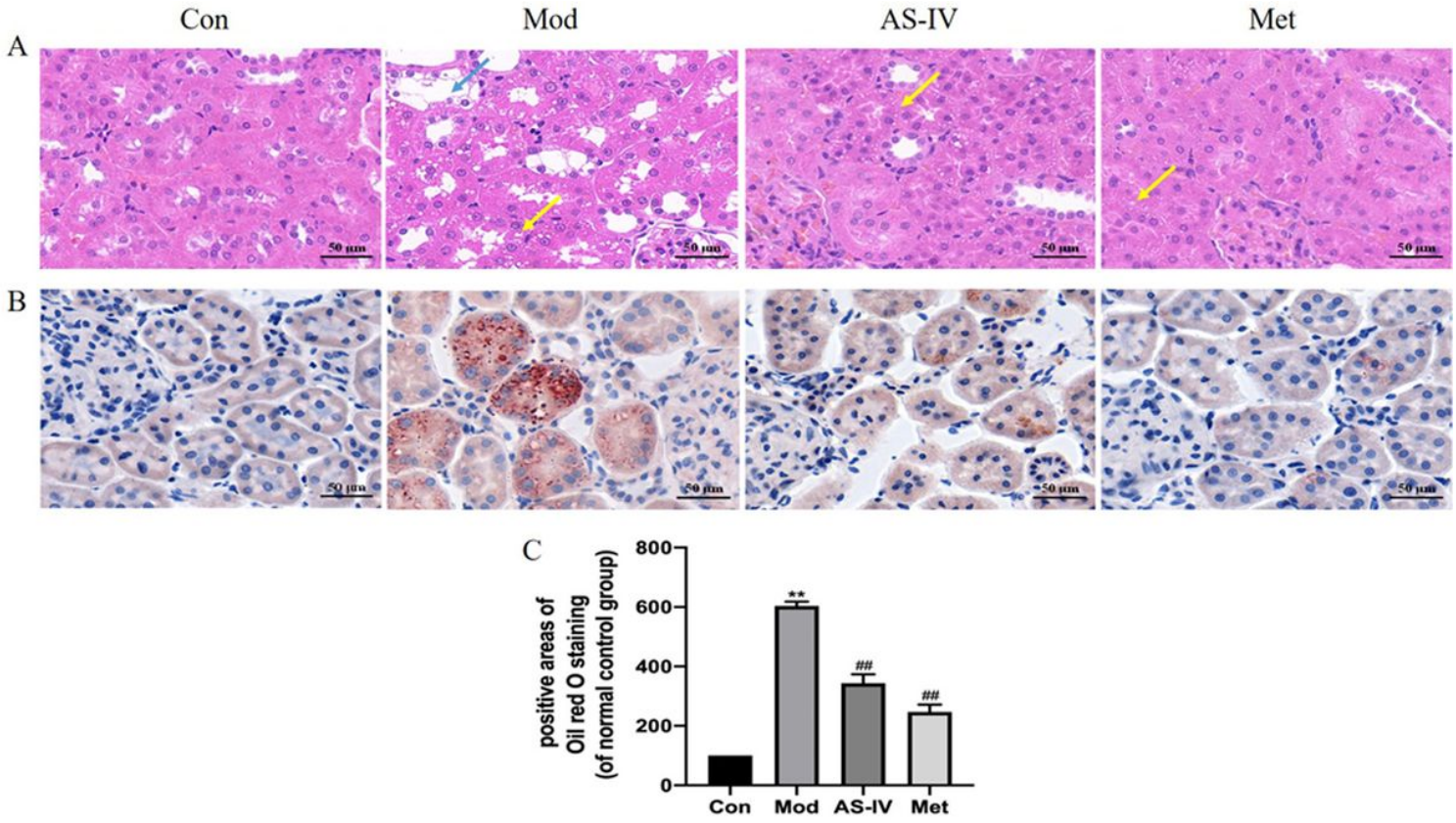

Figure 8

Effect of AS-IV treatment on renal histopathology and lipid deposition in T2DM rats. (A) The effect of AS-IV treatment on renal histopathology in T2DM rats (H&E staining, 400×). (B) The effect of AS-IV treatment on lipid deposition in T2DM rats (Oil red O staining, 400×). (C) Quantitative analysis of lipid deposition. Bars are represented as the means ± SD, n = 5. **P<0.01 compared with control group; ##P<0.01 compared with model group.

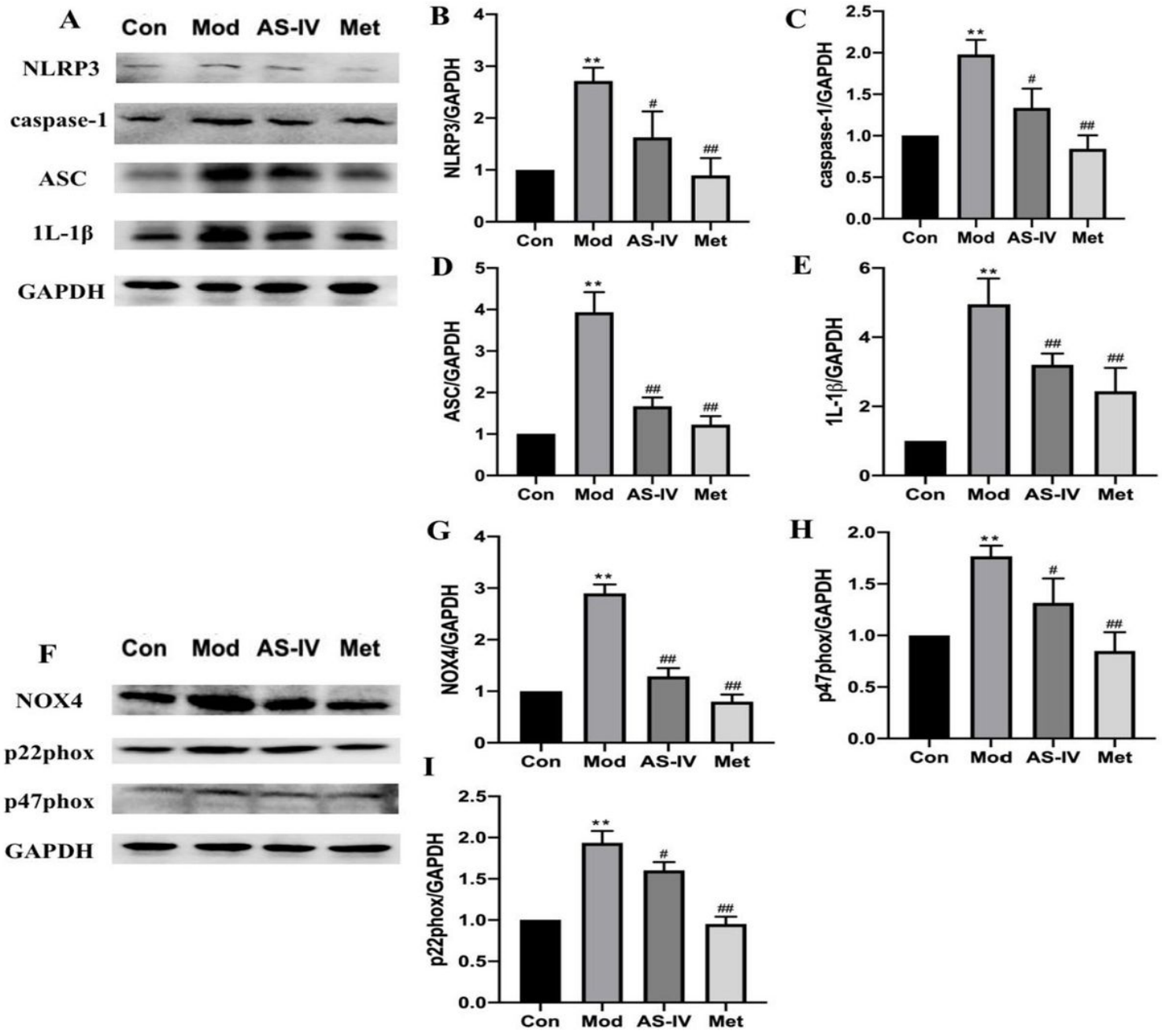

Figure 9

Effect of AS-IV treatment on expressions of NLRP3, ASC, caspase-1, IL-1β, NOX4, p22phox and p47phox in renal cortex of T2DM rats (Western blot). (A) The results of NLRP3, ASC, caspase-1 and IL-1β expressions. (B-E) Quantitative analysis of the expressions of NLRP3, ASC, caspase-1 and IL-1β. (F) The results of NOX4, p22phox and p47phox expressions. (G-I) Quantitative analysis of the expressions of NOX4, p22phox and p47phox. Bars are represented as the means ± SD, n=3. **P<0.01 versus the control group; #P<0.05, ##P<0.01 versus the model group.

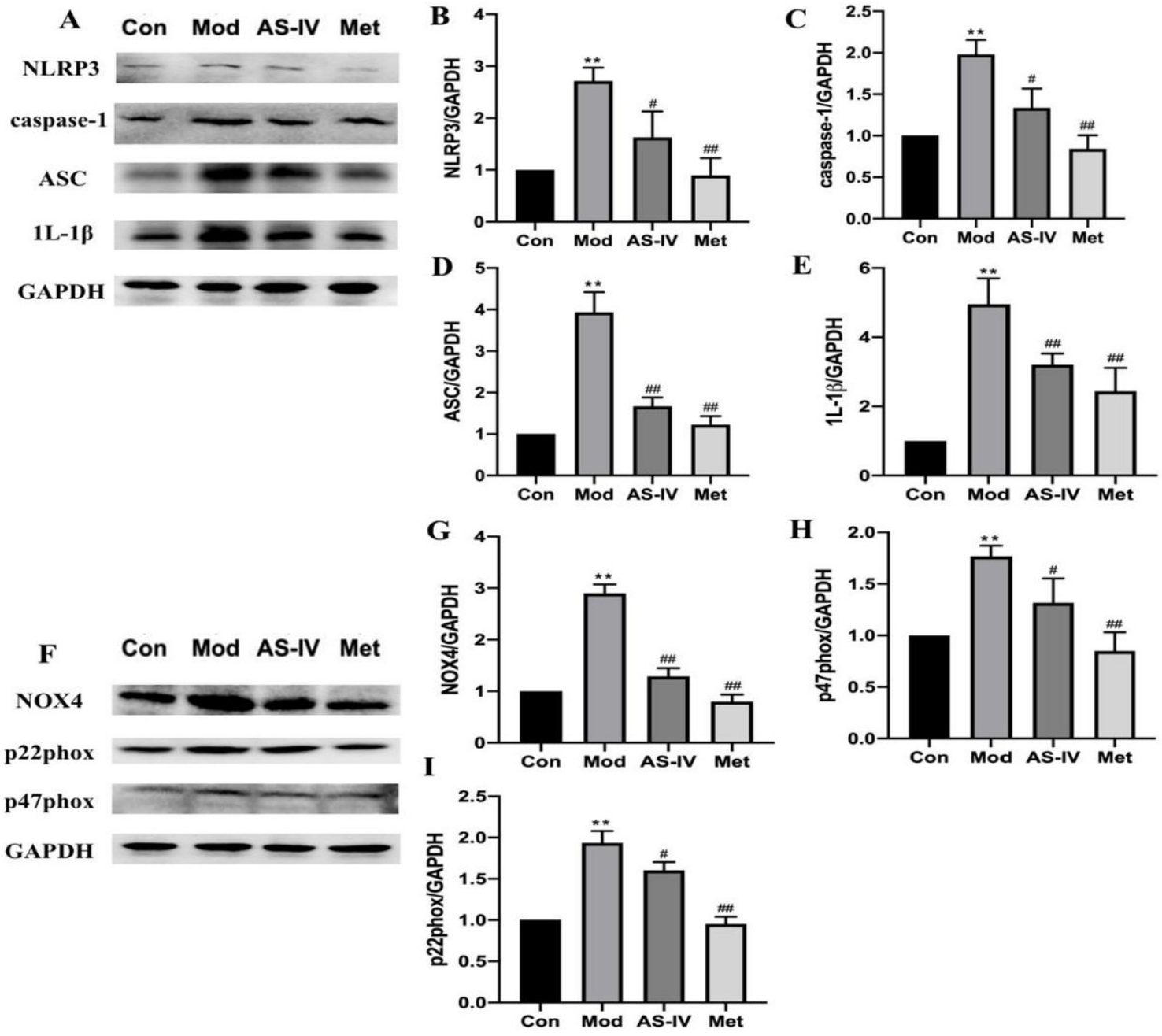

Figure 9

Effect of AS-IV treatment on expressions of NLRP3, ASC, caspase-1, IL-1β, NOX4, p22phox and p47phox in renal cortex of T2DM rats (Western blot). (A) The results of NLRP3, ASC, caspase-1 and IL-1β expressions. (B-E) Quantitative analysis of the expressions of NLRP3, ASC, caspase-1 and IL-1β. (F) The results of NOX4, p22phox and p47phox expressions. (G-I) Quantitative analysis of the expressions of NOX4, p22phox and p47phox. Bars are represented as the means ± SD, n=3. **P<0.01 versus the control group; #P<0.05, ##P<0.01 versus the model group.

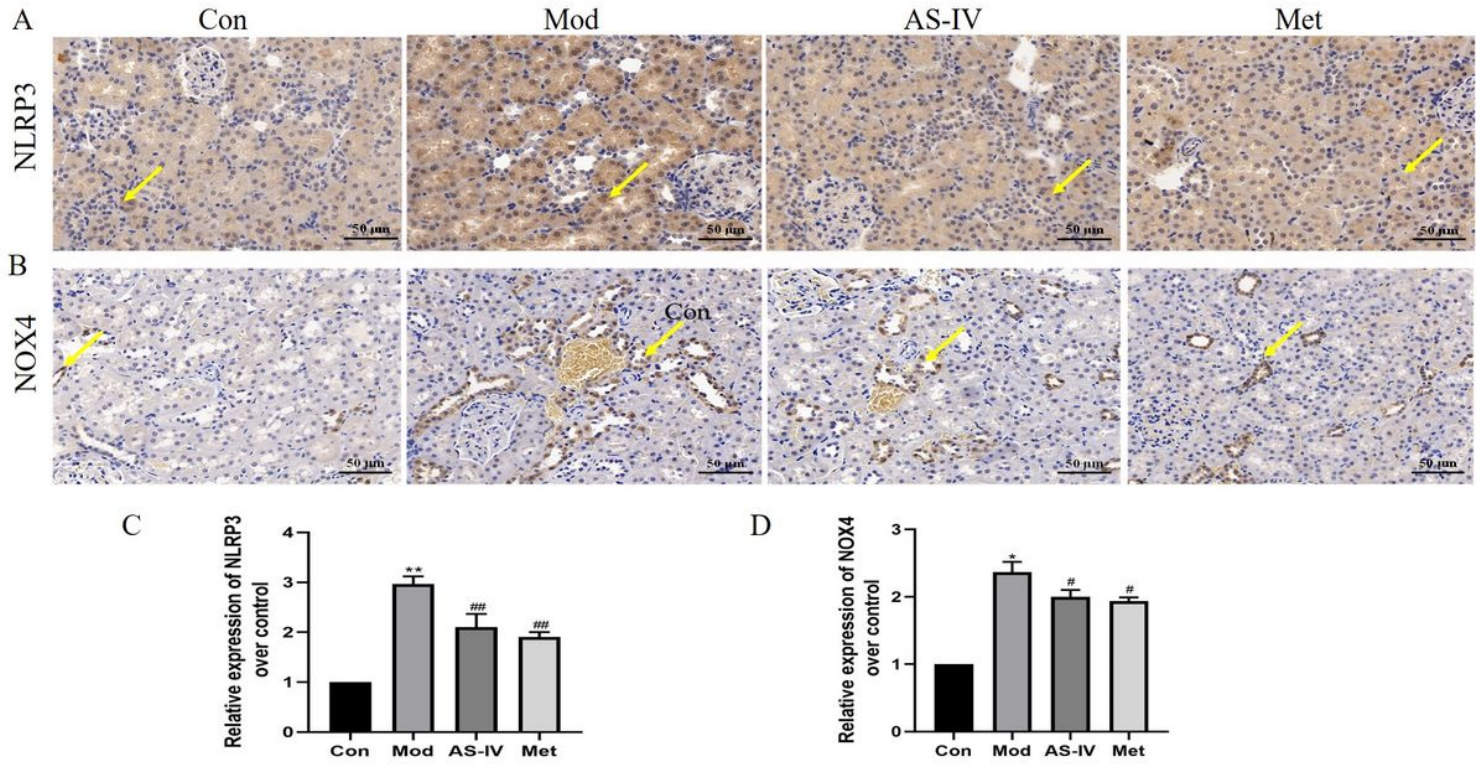

Figure 10

Effect of AS-IV treatment on expressions of NLRP3 and NOX4 in renal tubules of T2DM rats (Immunohistochemical staining, 400×). (A&B) The results of NLRP3 and NOX4 expressions in kidney tubules. (C&D) Quantitative analysis of NLRP3 and NOX4 expressions in kidney tubules. Bars are represented as the means ± SD, n=4. *P<0.05, **P<0.01 versus the control group; #P<0.05, ##P<0.01 versus the model group.

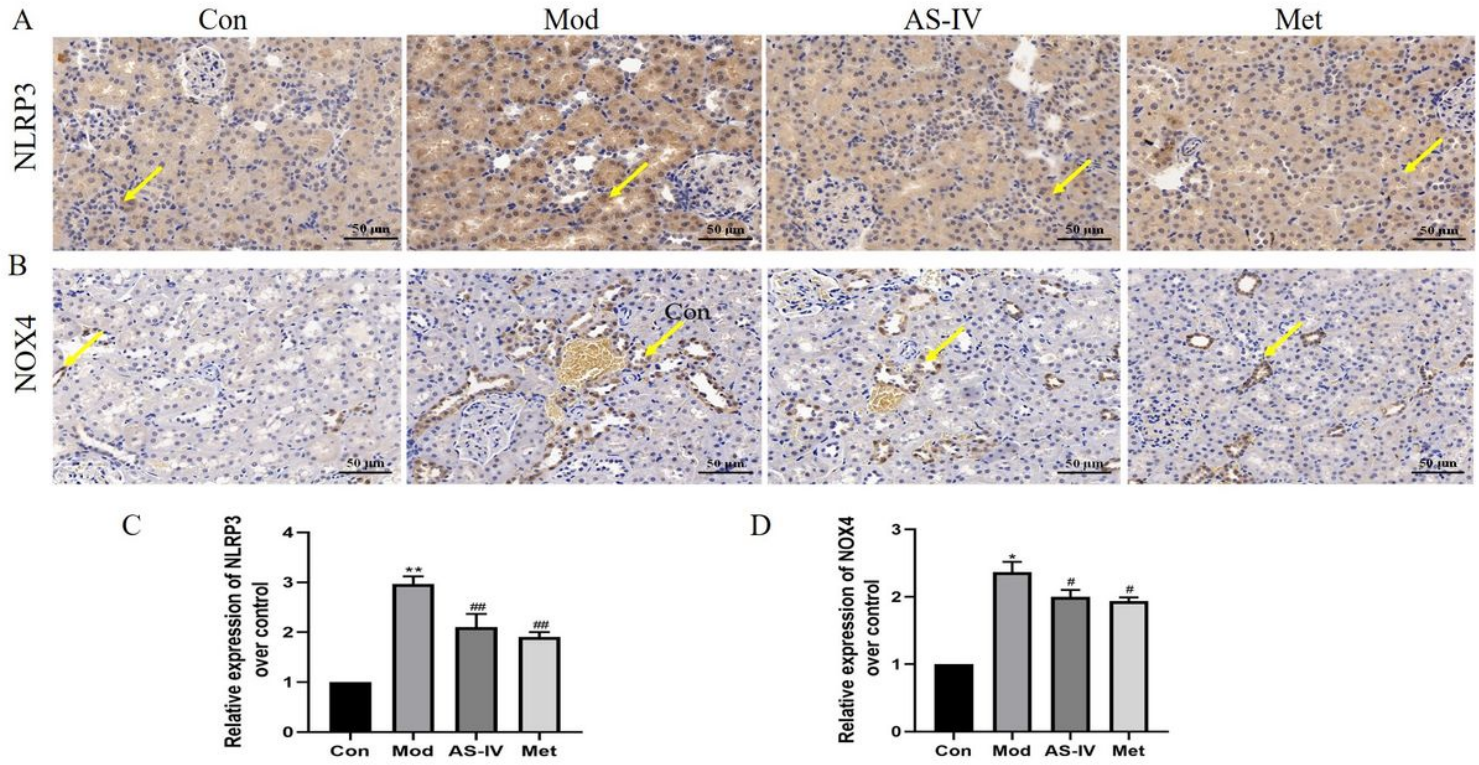

Figure 10

Effect of AS-IV treatment on expressions of NLRP3 and NOX4 in renal tubules of T2DM rats (Immunohistochemical staining, 400×). (A&B) The results of NLRP3 and NOX4 expressions in kidney tubules. (C&D) Quantitative analysis of NLRP3 and NOX4 expressions in kidney tubules. Bars are represented as the means ± SD, n=4. *P<0.05, **P<0.01 versus the control group; #P<0.05, ##P<0.01 versus the model group.